Supplementary Appendix to:

Multisystem Inflammation and Susceptibility to Viral infections in Human ZNFX1 Deficiency

Stefano Vavassori, Ph.D.[1#], Janet Chou, M.D.[2#], Laura Eva Faletti, Ph.D.[3#], Veronika Haunerdinger, Ph.D.[4], Lennart Opitz, M.S.[5], Pascal Joset, Ph.D.[6], Christopher J. Fraser, M.D.[7], Seraina Prader, M.D.[1], Xianfei Gao, M.D.[8], Luise A. Schuch, M.S.[8], Matias Wagner, M.D.[9], Julia Hoefele, M.D.[9], Maria Elena Maccari, M.D.[3], Ying Zhu, Ph.D.[10], George Elakis, B.Sc.[10], Michael T. Gabbett, M.D.[11], Maria Forstner, M.D. [8], Heymut Omran, M.D.[12], Thomas Kaiser, M.D.[12], Christina Kessler, M.D.[12], Heike Olbrich, Ph.D.[12], Patrick Frosk, M.D., Ph.D.[13], Abduarahman Almutairi, M.D.[2, 14], Craig D. Platt, M.D., Ph.D.[2], Megan Elkins, M.Sc.[2], Sabrina Weeks, B.A.[2], Tamar Rubin, M.D.[15], Raquel Planas, Ph.D.[1], Tommaso Marchetti, M.S.[1], Danil Koovely, M.S.[1], Verena Klämbt, M.D.[16], Neveen A Soliman, M.D., Ph.D.[17], Sandra von Hardenberg, Ph.D.[18], Christian Klemann, M.D.[19], Ulrich Baumann, M.D.[19], Dominic Lenz, M.D.[20], Andreas Klein-Franke, M.D.[21], Martin Schwemmle, Ph.D.[22], Michael Huber, Ph.D.[23], Ekkehard Sturm, M.D., Ph.D.[24], Steffen Hartleif, M.D.[24], Karsten Häffner, M.D.[25], Charlotte Gimpel, MB BChir MA [25], Barbara Brotschi, M.D.[26], Guido Laube, M.D.[27], Tayfun Güngör, M.D.[4], Michael F. Buckley, M.D.[10], Raimund Kottke, M.D.[28], Christian Staufner, M.D.[20], Friedhelm Hildebrandt, M.D.[16], Simone Reu-Hofer, M.D.[29], Solange Moll, M.D.[30], Achim Weber, M.D.[31], Hundeep Kaur, Ph.D.[32], Stephan Ehl, M.D.[3], Sebastian Hiller, Ph.D.[32], Raif Geha, M.D.[2*], Tony Roscioli, M.D., PhD.[10, 33, 34, 35*], Matthias Griese, M.D.[8*], Jana Pachlopnik Schmid, M.D., Ph.D.[1, 36*]

(1) Division of Immunology and Children's Research Center, University Children's Hospital Zurich, Zurich, Switzerland
(2) Division of Immunology, Boston Children's Hospital, Harvard Medical School, Boston, United States
(3) Institute for Immunodeficiency, Center for Chronic Immunodeficiency, Medical Center, Faculty of Medicine, University of Freiburg, Freiburg, Germany
(4) Division of Stem Cell Transplantation and Children's Research Center, University Children's Hospital Zurich, Zurich, Switzerland
(5) Functional Genomics Center Zürich, University of Zurich, ETH Zurich, Zurich, Switzerland
(6) Institute of Medical Genetics, University of Zurich, Schlieren, Switzerland
(7) Queensland Children's Hospital, South Brisbane, Queensland, Australia
(8) Division of Pediatric Pneumology, Dr. von Hauner Children's Hospital, University Hospital Munich, German Center for Lung Research (DZL), Munich, Germany
(9) Institute of Human Genetics, Klinikum rechts der Isar, School of Medicine, Technical University of Munich, Munich, Germany
(10) New South Wales Health Pathology Genomics, Prince of Wales Hospital, Sydney, Australia

(11) Centre for Genomics and Personalised Health, School of Biomedical Sciences, Queensland University of Technology, Brisbane, Australia
(12) Clinic for General Pediatrics, University Hospital Münster, Münster, Germany
(13) Division of Clinical Immunology and Allergy, Department of Pediatrics and Child Health, University of Manitoba, Winnipeg, Canada
(14) Department of Pediatrics, Security Forces Hospital, Riyadh, Saudi Arabia
(15) Division of Pediatric Clinical Immunology and Allergy, Department of Pediatrics and Child Health, University of Manitoba, Winnipeg, Canada
(16) Division of Nephrology, Harvard Medical School, Boston Children's Hospital, Boston, USA
(17) Department of Pediatrics, Center of Pediatric Nephrology and Transplantation, Cairo University, Cairo, Egypt
(18) Department of Human Genetics, Hannover Medical School, Hannover, Germany
(19) Department of Paediatric Pulmonology, Allergy and Neonatology, Hannover Medical School, Hannover, Germany
(20) Division of Neuropediatrics and Pediatric Metabolic Medicine, Center for Pediatric and Adolescent Medicine, University Hospital Heidelberg, Heidelberg, Germany.
(21) Division of Pediatric Hematology and Oncology, Cantonal Hospital Aarau, Aarau, Switzerland
(22) Institute of Virology, Medical Center - University of Freiburg, Freiburg, Germany; Faculty of Medicine, University of Freiburg, Freiburg, Germany
(23) Institute of Medical Virology, University of Zurich, Zurich, Switzerland
(24) Division of Pediatric Gastroenterology and Hepatology, University Hospital Tübingen, Tübingen, Germany
(25) Department of Internal Medicine IV (Nephrology), University Medical Center Freiburg, Faculty of Medicine, University of Freiburg, Germany
(26) Department of Pediatric and Neonatal Intensive Care, University Children's Hospital Zurich, Zurich, Switzerland
(27) Division of Nephrology, University Children's Hospital Zurich, Zurich, Switzerland; Prof. Dr. G. Laube is now at the Cantonal Hospital Baden, Baden, Switzerland
(28) Division of Neuroradiology, Department of Diagnostic Imaging and Intervention, University Children's Hospital Zurich, Zurich, Switzerland
(29) Institute of Pathology, University of Würzburg, Würzburg, Germany
(30) Department of Pathology and Immunology, University of Geneva, Geneva, Switzerland
(31) Department of Pathology and Molecular Pathology, and Institute of Molecular Cancer Research (IMCR), University Hospital and University Zurich, Zurich, Switzerland
(32) Biozentrum, University of Basel, Basel, Switzerland
(33) Centre for Clinical Genetics, Sydney Children’s Hospital, Randwick, NSW, Sydney, Australia
(34) Prince of Wales Clinical School, University of New South Wales, Sydney, Australia

(35) Neuroscience Research Australia (NeuRA), University of New South Wales, Sydney, Australia
(36) Pediatric Immunology, University of Zurich, Zurich, Switzerland

#Joint First Authors
*Joint Senior Authors

Corresponding authors:
Dr. Jana Pachlopnik Schmid, Division of Immunology, University Children's Hospital Zurich, Steinwiesstr. 75, 8032 Zurich, Switzerland, jana.pachlopnik@kispi.uzh.ch.
Dr. Raif Geha, Division of Immunology, Boston Children's Hospital, Harvard Medical School, Boston, United States, Geha, raif.geha@childrens.harvard.edu.

CONTENT:

1. AUTHOR CONTRIBUTIONS

SV designed and performed experiments and wrote the manuscript. JC and LEF designed and performed experiments and contributed to writing of the manuscript. VH performed experiments. LO performed bioinformatics analyses of exome sequencing and transcriptomic data. PJ performed genetic analyses and initiated international collaboration. CJF and SP contributed to data collection, patients' care and writing of the manuscript. XG contributed to data collection. MG, JH and LAS contributed to data collection and genetic analysis. MEM contributed to data collection and patients' care. YZ, HOm, TK, HOl, and PF performed genetic analyses. GE and MTG contributed to data collection. MF, CG, CK, and UB contributed to data collection and patients' care. CK and TR contributed to data collection from patients. TR, VK, CP, AA and SvH contributed to genetic analyses and data collection from patients. RP and TM performed flow cytometry experiments. DK, ME and SW contributed to experiments. NAS and DL contributed to data collection and patients' care. AKF, ES, SH, KH, MFB, FH, TG, GL, BB, and CS contributed to patients' care. MH performed viral metagenomic analyses. SE contributed to the design of experiments, data interpretation and patients' care. RK performed the assessment of neuro-radiological images. SR performed histological analysis of lung tissue. SM performed histological analysis of kidney tissue. HK and SH performed protein structure prediction modelling. AW performed histological analysis of liver tissue. RG contributed to data interpretation and writing of the manuscript. TR performed genetic analyses, contributed to data collection and writing of the manuscript. MG contributed to patients' care, project initiation via the chILD-Eu registry and biobank, data collection and writing of the manuscript. JPS set up the Genetic Study of Immunodeficiency, contributed to patients' care, data collection, wrote the manuscript and coordinated the study. All authors critically read, revised and approved the final version of the manuscript.

2. SUPPLEMENTARY MATERIAL AND METHODS

Study participants

The patients were enrolled in ongoing, institutional–review–board (IRB)–approved studies of monogenic diseases at the Prince of Wales Hospital (Randwick, Australia: IRB references 13/094 and LNR/13/SCHN/112), the University Hospital Münster (Münster, Germany: IRB reference: AZ 2012-373-f-S), the University of Munich (Munich, Germany; ClinicalTrials.gov. NCT02852928; IRB reference: EK 111-13, 20-329), the Hannover Medical School (Hannover, Germany; IRB reference: EK 8657_BO_K_2019), the Boston Children's Hospital (Boston, United States IRB reference: 04-09-113R), and the Division of Immunology at the University Children's Hospital Zurich (Zurich, Switzerland; ClinicalTrials.gov. NCT02735824; IRB reference: PB_2016_02280). For the definition of HLH, the HLH-2004 study group criteria have been used (1). For the definition of acute liver failure, the PALF study group criteria have been used (2)

Next-generation sequencing and variant annotation

Next-generation sequencing was performed and analyzed at New South Wales Health Pathology (NSWHP) Randwick Genomic Laboratory (Sydney, Australia) using either Illumina or Thermo Fisher platforms, as described previously (3). Data were filtered using an in-house genomic annotation and interface application (GAIA), which overlies GEMINI v20.1 and has been approved by the National Association of Testing Authorities, Australia (4). Reads were aligned with the Human Genome Reference Sequence hg19/GRCh37 and single nucleotide and short indel variants were called as described previously (3).

Variant quality was assessed using quality score recalibration and the variants were then annotated using the Ensembl Variant Effect Predictor (http://www.ensembl.org/info/docs/tools/vep/index.html). Targeted-exome sequencing of genomic DNA was performed at the Cologne Center for Genomics (Cologne, Germany). Agilent SureSelect (version 6-r2) was used for enrichment. Enriched preparations were sequenced with the HiSeq2000 platform (Illumina) as paired-end 2 × 100 bp reads. The proportion of 30× coverage in the targeted regions was greater than 80%. In order to identify relevant mutations, a whole-genome homozygosity mapping and exome sequencing strategy was applied to kindreds 1 and 5.

Variant prioritization and classification

Variants that were too frequent to cause a fully penetrant Mendelian disorder were de-prioritized, with a threshold frequency (based on the Exome Aggregation Consortium, gnomAD, the 1000 Genomes Project, and the NSWHP in-house database) of >2% for homozygous and compound heterozygous inheritance models and >0.1% for heterozygous inheritance models. Variants predicted to have a low impact on protein function by the GEMINI software tool were also de-prioritized (4). Each of the remaining rare variants were reviewed by skilled analysts and classified according to the American College of Medical Genetics and Genomics guidelines (5) as subsequently modified (6, 7) to incorporate aspects of the scoring system reported by Karbassi et al (8). Variant quality was checked by inspecting the sequence data after binary sequence alignment map (.bam) files had been uploaded into the Integrative

Genomics Viewer (9). The following parameters were analyzed for each variant: the type of mutation (null/truncating, missense, synonymous, in-frame deletion variant, etc.), zygosity, inheritance pattern, frequency in the population, allele case frequency (from disease-specific publications and ClinVar), conservation, protein/domain structure, associated phenotypes, predicted pathogenicity (in SIFT, PolyPhen2, CADD, and ClinPred), functional/animal studies, and the disease's mutation spectrum. Genematcher was used as to connect the investigators, on the basis of their common interest in the candidate gene *ZNFX1* (10)

Statistical analysis

Two-way ANOVA, Sidak's multiple comparisons test was used. Non liner regression and half-life ware calculated using exponential (Malthusian) growth. All statistical analyses were performed with GraphPad Prism software (version 8.4.2, GraphPad Inc., La Jolla, CA).

Prediction of protein homology model

Domains were searched for with the NCBI CDD database 4-6, and the protein similarity search was performed with HHPred7 (11-14). The Walker A motif was matched to the consensus sequence (G/A)XXXXGK(T/S)Y, and zinc fingers were matched to the sequence C-X(1-6)-H-X-C-X3-C(H/C)-X(3-4)-(H/C)-X(1-10)-C. The hit with the greatest sequence coverage versus the X-ray structure (PDB ID: 4PJ3) was used as a template model for ZNFX1 from residues 183 to 1255, using MODELLER8 (15). The homology structure was viewed and analyzed with PyMOL9 (16).

Tissue expression

The Human MTC Panel I and Human Immune System MTC Panel (Takara) were used as normalized, first-strand cDNA library preparations from RNA extracted from the indicated tissues. The following TaqMan probe/primer sets (Thermo Fisher Scientific) were used: Hs99999901 for 18S, and Hs01105231 for ZNFX1 in combination with the TaqMan Fast Advance Master Mix (Thermo Fisher Scientific). The qPCR assay was carried out on a C1000 Touch™ thermal cycler equipped with a CFX384 Touch™ real-time detection system (Bio-Rad).

Transcriptomic profiling

mRNA was isolated from control and patient fibroblasts, stimulated as indicated. cDNA then synthesized from 10 ng of total RNA using SuperScript™ VILO™ cDNA Synthesis Kit (11754050, ThermoFisher Scientific). Barcoded libraries were prepared using the Ion AmpliSeq Transcriptome Human Gene Expression Kit as per the manufacturer's protocol and sequenced using an Ion S5TM system. Differential gene expression analysis was performed using the ampliSeqRNA plugin (ThermoFisher). Pathway analysis was done using Ingenuity Pathway Analysis (Qiagen) and Gene Set Enrichment Analysis, using adjusted p values of <0.01 and fold-change greater than 1.5 or less than -1.5.

Fibroblast stimulation assay

Primary human dermal fibroblasts were grown in Dulbecco's Modified Eagle Medium (DMEM) (Thermo Fisher Scientific) supplemented with 10% fetal bovine serum (FBS). The cells were transfected with poly(dA:dT)/LyoVec and poly(I:C)(HMW)/LyoVec, or treated with soluble poly(I:C)(HMW) (Invivogen), according to manufacturer guidelines. Briefly, 500 ng/ml of poly(dA:dT)Lyovec, poly(I:C)HMW-LyoVec or poly(I:C)HMW were added to 75% confluent dermal fibroblast cultures. At the indicated time point, the culture medium was removed and the cells were resuspended in Trizol reagent (Thermo Fisher Scientific) for RNA isolation.

For transcriptomic analysis primary dermal fibroblasts from patients and controls were stimulated with 3 µg/mL of poly(I:C)HMW or transfected with 3 µg/mL of Lyovec-poly(I:C)HMW or 3 µg/mL Lyovec-poly(dA:dT) (Invivogen).

Viral infection assay.

PBMCs from patients and healthy donors (CTRL) were pre-treated with different concentrations of Lyovec-poly(I:C)HMW for 12 hours followed by infection with VSV-GFP. Five hours after infection, cells were harvested and GFP expression measured on monocytes by flow cytometry.

Detection of ZNFX1 by Western blotting

Primary dermal fibroblasts were lysed in RIPA buffer (Thermo Fisher Scientific) supplemented with MINI protease inhibitor cocktail (Roche) under resting conditions or 24 h after transfection with 0.5 µg/ml poly(dA:dT)/LyoVec or 0.5 µg/ml poly(I:C)(HMW)/LyoVec (Invivogen), as described above. Protein concentrations were assayed using Bradford's method (Bio-Rad). Next, 20 µg of protein extracts were resolved on Criterion TGX 4-15% precast gels (Bio-Rad) and transferred to PVDF membranes using Trans-Blot Turbo (Bio-Rad). ZNFX1 was detected with rabbit-mAb (Abcam, clone EPR12330) and HRP-conjugated goat anti-rabbit antibody (Thermo Fisher Scientific). As a loading control, actin was detected with rhodamine-conjugated anti-actin heavy antigen-binding fragment (Bio-Rad). Images were acquired with the Chemidoc MP system (Bio-Rad) and analyzed with Image Lab software (version 6.0.1, build 34, Standard Edition; Bio-Rad).

RNA isolation

Blood samples from patients and their parents were collected in PAXgene tubes (BD Biosciences) and RNA was isolated using the PAXgene System. RNA from dermal fibroblasts cultures was isolated using the Trizol Plus RNA Isolation Kit (Thermo Fisher Scientific).

Quantitative polymerase chain reaction (qPCR)

RNA was reverse-transcribed using the Superscript IV Vilo Master Mix (Thermo Fisher Scientific), according to the manufacturer's instructions. The following TaqMan probe/primer (Thermo Fisher Scientific) sets were used: Hs99999901 for 18S, Hs0089508 for MX1, NH 027866424 for GAPDH, Hs00973635 for OAS1, Hs001966324 for OAS3 and Hs00942643 for OAS2, in combination with the TaqMan Fast Advance Master Mix (Thermo Fisher Scientific). The qPCR assay was carried out on a C1000 Touch^{TM} thermal cycler equipped with a CFX384

Touch™ real-time detection system (Bio-Rad). Data were analyzed using CFX Maestro 1.1 software (Bio-Rad).

RNA stability assay

Dermal fibroblasts were plated in 24-well tissue culture plates and transfected with 500 ng/ml Lyovec-poly(dA:dT), as described above. Eighteen hours later, 500 µg/ml of the polymerase II inhibitor 5,6-dichlorobenzimidazole 1-β-D-ribofuranoside (Merck) was added to the cultures. At the indicated time points, the growth medium was removed, and the cells were resuspended in Trizol reagent (Thermo Fisher Scientific) for RNA isolation.

Metagenomic viral sequencing:

Viral metagenomic sequencing was performed as previously described (Kufner et al. Two Years of Viral Metagenomics in a Tertiary Diagnostics Unit: Evaluation of the First 105 Cases. genes 10, 2019). Briefly, samples were pre-processed upon arrival and nucleic acid extracts were collected, followed by reverse transcription with random hexamers and second strand synthesis. Sequencing libraries were constructed using the NexteraXT protocol (Illumina, San Diego, CA, USA) and sequenced on an Illumina MiSeq for 1 x 151 cycles using version 3 chemistry. Analysis was performed using the in-house pipeline VirMet.

ZNFX1 overexpression:

Dermal fibroblasts were transfected with pFN21A-ZNFX1 (Promega) together with pcDNA6.2/EmGFP-Bsd/V5-DEST (Thermofisher). Transfectants were then selectively enriched in DMEM-10%FBS medium supplemented with blasticidin for three days, followed by one day resting in plain medium prior to stimulation. Viability of transfectants was assessed by measurement of Caspase 3, Caspase 8 and Caspase 9 in a fluorometric multiplex activity assay (Abcam). Transfection efficiency following selective enrichment was over 65% as assessed by flow cytometric analysis after staining of HaloTag with the HaloTag-TMR ligand (Promega).

3. SUPPLEMENTARY PATIENT CLINICAL HISTORIES

Kindred 1. P1.1, P1.2 and P1.3 were born to consanguineous parents of Arabic origin. **P1.1** (the parents' first child) was born in Iraq. She presented with failure to thrive from birth onwards, severe general weakness, and hepatitis. At the age of 6 months, she developed recurrent pneumonia and anemia; a clinical examination revealed lymphadenopathy and hepatomegaly. The patient died at the age of 2.7 years.

Her 1.5 year younger sister (**P 1.2**, the index patient) presented with afebrile seizures at the age of 6 months. A second seizure (with a normal EEG) occurred one month later and was followed by a first episode of pneumonia. Due to recurrent lung infections, she developed chronic lung disease, with evidence of cholesterol pneumonitis on a lung biopsy. Tuberculin conversion was diagnosed at the age of 9 months and treated with isoniazid.

At the age of 1.5 years, the seizures became frequent (once a week) and anticonvulsant medication (oxcarbazepine) was initiated. At that time, she had short stature, palmar erythema, hepatosplenomegaly, and finger clubbing.

At 3 years of age, chronic polyarthritis was diagnosed, with recurrent arthritic swelling of the hips, knees, and elbows. The patient was treated with steroids, methotrexate and azathioprine. Failure to thrive worsened, and abdominal pain appeared. Homozygous lactase deficiency was diagnosed, although a reduction in lactose intake did not completely abolish the symptoms. At the same time, mediastinal and hilar lymphadenopathy developed.

At 7 years of age, the patient had a severe H1N1 pneumonia. She had moderate to severe restrictive lung function impairment.

At 8 years of age, the patient developed a right and left ventricular dilatation developed as a result of pulmonary hypertension. Due to a progressive decline in lung function and respiratory failure, the patient underwent lung transplantation at the age of 10 years. Bronchiolitis obliterans developed after the transplantation.

A year later, a lung biopsy revealed post-transplant lymphoproliferative disease.
At the age of 13, liver infection with *Mycobacterium kansasii* was diagnosed on a liver biopsy, with extensive lymphoid infiltrations and granulomatous reactions.

One year later, the patient developed hypothyroidism, and thyroid hormone replacement therapy was initiated. At the same age, the patient's lung function started to decrease rapidly, and a repeat transplant was considered. However, this was ruled out by a severe concomitant adenovirus infection, and the patient died of respiratory failure. The autopsy demonstrated chronic necrotizing pulmonary aspergillosis, diffuse alveolar damage, and hepatic sinusoidal dilatation.

P1.3 (P1.2's brother, 6 years younger) was born in Germany and presented with hypoxemia, prolonged and severe jaundice, and failure to thrive soon after birth. Tetralogy of Fallot and patent foramen ovale were diagnosed; cardiac catheterization was performed at the age of 1 month. Concurrently, the child developed recurrent thrombocytopenia (24 G/L) without any evidence of sepsis. A lung biopsy obtained during cardiac surgery showed cellular interstitial pneumonitis, which was treated with azathioprine and prednisolone. At the age of 5 months, the patient developed a respiratory tract infection with hepatosplenomegaly.

Intestinal invagination was observed at 6 months of age, and ileocecal resection was necessary. The biopsy showed an inflammatory conglomerate tumor in the right lower abdominal area, with a distended appendix.

At this time, the patient's transaminase level rose sharply (ASAT: 3145 U/l; ALAT: 833 U/l). He had fever, hepatosplenomegaly, transfusion-dependent anemia, thrombocytopenia, coagulopathy (with a requirement for fresh frozen plasma), mild elevation of triglycerides (3.32 mmol/l) and an elevated serum soluble IL-2 receptor level (sIL-2R, 2957 U/ml); as such, he met the diagnostic criteria for haemophagocytic lymphohistiocytosis (HLH). One month later, a liver biopsy was taken but did not show any evidence of metabolic disease.

At the age of 11 months, further tests showed that the bone marrow cellularity was normal, with no evidence of natural killer cell dysfunction or cytotoxicity defects.

At the age of 13 months, the patient started to experience afebrile generalized seizures. He died at the age of 14 months from a severe H1N1 pneumonia infection with acute respiratory distress syndrome (ARDS) and cardiorespiratory failure.

Kindred 2. P2.1 and P2.2 were born to non-consanguineous parents of Caucasian origin. **P2.1** had an uneventful medical history including normal tolerance of MMR vaccination until the age of 4 years, when she presented with persistent microhematuria, microalbuminuria, pneumonia, and gastroenteritis. She was hospitalized with arterial hypertension, mild thrombocytopenia (123 G/L), proteinuria, hypochromic microcytic anemia, and elevated LDH levels (1050 U/L). A kidney biopsy showed thrombotic microangiopathy (TMA). An atypical hemolytic-uremic syndrome was diagnosed, and genetic testing revealed a homozygous deletion in *CFHR1*/*CFHR3*. Antihypertensive medication normalized the patient's blood pressure but her first morning urine remained positive for microhematuria (without proteinuria).

Between the age of 4 and 8 years, she had repeated hospitalizations (once per year, for a week) for episodes with high fever, pneumonia, lethargy, elevated transaminases. Since then, no other relevant infections or inflammatory states/diseases occurred, but she maintained persistent elevation of liver enzymes. At the age of 10, ultrasound showed a focal isoechogenic, homogeneous, hepatic lesion (1.7×1.4 cm) in segment IV. Nodular regenerative hyperplasia was diagnosed, following a liver biopsy.

At last follow-up, the patient was in a stable condition, with normal blood pressure, intermittent microalbuminuria, persistent microhematuria, and slightly elevated transaminases.

P2.1's brother (**P2.2**) was born with microcephaly and suffered from recurrent infections from the first week of life onward. At the age of 3 months, following rotavirus vaccination, he experienced an episode of respiratory syncytial virus (RSV) bronchitis, together with thrombocytopenia and increased transaminases. He recovered but was re-admitted 2 weeks later again for RSV bronchitis, thrombocytopenia, and elevated transaminases. At this time, elevated TSH was detected and thyroid hormone treatment was administered. Brain MRI was normal.

At the age of 4 months, the patient developed fever. A clinical examination detected hepatosplenomegaly, and abdominal ultrasound showed ascites. P2.2 had pronounced thrombocytopenia (9 G/L), anemia (hemoglobin: 60 G/L), elevated transaminases (ASAT:

10521 U/L; ALAT: 2472 U/L), elevated LDH (13230 U/L), and a coagulation disorder (prothrombin 20%; prothrombin time (PTT): 68 sec; antithrombin <25%). Acute liver failure and influenza A virus infection were diagnosed. Despite intensive care, the patient's respiratory status deteriorated, and acute kidney failure occurred. The patient died of multi-organ failure.

Kindred 3. P3.1 and P3.2 were born to consanguineous Syrian parents (cousins). Their three older siblings were in good health. **P3.1** had experienced recurrent seizures and thrombocytopenia in Syria. After a prolonged generalized seizure, cardiac arrest occurred, and she died at the age of 5 months.

At the age of 10 months, **P3.2** was admitted to hospital with fever and an upper respiratory tract infection. Laboratory work-up revealed thrombocytopenia (71 G/L), elevated transaminases (ASAT: 452 U/l; ALAT: 229 U/l) and elevated D-dimers (1619 µg/L). Lumbar puncture showed 6 cells/µl, an elevated protein level (385 mg/L), and normal lactate and glucose levels in the CSF. The patient was treated with antibiotics and his clinical situation improved.

One month later, he was re-admitted with suspected gastroenteritis, again associated with thrombocytopenia (70 G/L) and elevated transaminases (ASAT: 158 U/l; ALAT: 73 U/l). His clinical condition improved upon symptomatic treatment, and he was again discharged in relatively good health.

Two weeks later, P3.2 was treated with oral antibiotics for otitis media. His condition did not improve and he became somnolent. The boy was admitted to hospital, where acute hepatic cytolysis (ASAT: 10217 U/L; ALAT: 2420 U/L; LDH: 7590 U/L) and liver dysfunction (international normalized ratio: 1.14), petechiae, and encephalopathy were noted. Ultrasound showed an enlarged, hyperechogenic liver with nodular areas; these features were compatible with a diagnosis of progressive liver fibrosis. He experienced a tonic-clonic seizure after admission, and was transferred to a pediatric liver transplant center where he developed progressive multi-organ failure. Brain MRI revealing massive necrotizing encephalitis and leptomeningeal enhancement. Follow-up MRI showed edema of both thalami, and disseminated ischemia in the periventricular white matter, the corpus callosum, and right cerebellum. Respiratory insufficiency prompted intubation but the patient's respiratory status worsened, with tracheal bleeding. Acute renal failure prompted the initiation of continuous venous hemofiltration. A CT scan revealed perturbed kidney perfusion that was consistent with a diagnosis of shock kidney. Empiric antibiotic and antimycotic treatment was initiated. Due to a massive blood load of HHV-6, ganciclovir/foscarnet treatment was initiated. Norovirus was found in the stools. Immunological work-up showed the transient absence of NK cells, an elevated sIL-2R level (2122 U/mL), and hyperferritinemia (2204 µg/dl).

The patient died at the age of 12 months due to multi-organ failure in the context of a severe, systemic HHV-6 infection.

Kindred 4. P4.1 and P4.2 were born to non-consanguineous parents of Caucasian origin. **P4.1** presented with seizures at the age of 7 months. She soon developed respiratory distress, and was admitted to hospital. Mechanical ventilation was required from day 2

onwards. Although the patient was not feverish, a clinical examination revealed hepatosplenomegaly and laboratory tests revealed anemia (hemoglobin: 67 g/l), thrombocytopenia (15 G/L), leukocytosis (white blood cell (WBC) count: 35.8 G/L, with a neutrophil left shift), elevated ferritin (4800 µg/L), elevated triglycerides (9.5 mmol/L), elevated ASAT (2500 U/L), hemophagocytosis (documented by a bone marrow aspirate), and CNS involvement (seizures, abnormal MRI findings, and elevated CSF protein levels (580 g/L)). Adenovirus DNA was detected in the patient's blood and nasopharyngeal aspirate and so cidofovir was initiated. Natural killer (NK) cell degranulation (as assessed by CD107a expression) was within the normal range, as was the perforin expression level, NK cell cytotoxicity, and sIL-2R level on day 3 post-admission. As the patient's clinical and laboratory profiles met the diagnostic criteria for HLH, treatment with dexamethasone, etoposide and cyclosporine was initiated (in line with the HLH2004 guidelines). Although the ferritin and triglyceride levels normalized, the patient remained dependent on platelet transfusions and then developed pulmonary hemorrhage with edema, ascites, and pleural effusions. Elevated creatinine levels, high blood pressure and left ventricular hypertrophy were also noted. A bone marrow aspirate collected on day 10 post-admission showed bone marrow aplasia without hemophagocytosis. On the same day, the patient's condition deteriorated in the context of *E.coli* sepsis. Despite the initiation of extracorporeal membrane oxygenation (ECMO), the patient died 24 hours later.

P4.2 (P4.1's brother) presented with cytopenia and hepatosplenomegaly at the age of 9 months, in the context of symptoms of a viral upper respiratory infection. However, a viral pathogen was not identified. A bone marrow aspirate was normal, and the respiratory infection resolved spontaneously. At the age of 22 months, P4.2 developed hepatosplenomegaly and nephrotic syndrome; this resulted in respiratory compromise requiring high-flow oxygen supplementation. Adenovirus and parainfluenza viruses were detected in the nasopharyngeal aspirate. An ultrasound assessment of the liver revealed a non-specific, coarse echotexture. A liver biopsy revealed vasculopathic changes with evolving nodular regenerative hyperplasia. Even though the patient recovered from this episode (following treatment with corticosteroids), developmental regression was observed from the age of 22 months onwards. Brain MRI revealed multifocal white matter changes in both hemispheres of the brain (on T2 and fluid attenuation inversion recovery (FLAIR) sequences); this was suggestive of significant, multifocal gliosis. Although a diagnosis of HLH was considered at the time of the second episode (i.e. at the age of 22 months), the patient did not meet all the criteria. The patient also had hypertension and left ventricular hypertrophy. Natural killer cell degranulation (as assessed by CD107a expression) was within the normal range, as were perforin expression, lymphocyte subset counts and immunoglobulin (IgA/M/G) levels. In view of the sibling's death and the signs of possible immune dysregulation, the patient underwent hematopoietic stem cell transplantation (HSCT) with a fully matched unrelated donor. At last follow-up (5 years after transplantation), the patient was in good health and had not experienced further episodes of immune dysregulation. Brain MRI showed that the white matter changes had stabilized 6 months after HSCT and had even regressed 5 years after HSCT. Although the patient has made developmental progress since the HSCT, he continues to show developmental delay and has been diagnosed with autism.

Kindred 5. P5.1 and P5.2 were born to non-consanguineous parents of Caucasian origin. At the age of almost 3 months, **P5.1** presented with fever, respiratory distress, and mild thrombocytopenia. Within 3 days of admission, the patient's condition deteriorated; he developed acute respiratory distress syndrome, bicytopenia, and kidney and liver failure. A clinical examination revealed hepatomegaly but no splenomegaly. Laboratory tests showed anemia (hemoglobin 75 g/l), thrombocytopenia (54 G/L), leukocytosis (WBC count: 43.7 G/L, neutrophilic granulocytes (20.1 G/L with a neutrophil left shift, lymphocyte count: 20.7 G/L), a coagulation disorder (PTT: 27% (normal values >70); INR: 2.82 (normal values <1.3); activated PTT: 93 s (normal values <50); factor V: 14% (normal values >60%); factor VII: 14%; (normal values >50); and fibrinogen: 0.78 g/l (in the normal range)), and elevated liver enzymes (ASAT: 13375 U/L; ALAT: 1456 U/L), LDH (18191 U/L), ferritin (81418 µg/L) and sIL-2R (3185 pg/ml). Human herpesvirus type 6 (HHV6) and cytomegalovirus (CMV) DNA was detected in the patient's blood ($8x10^5$ copies/ml and 2.4×10^3 copies/ml, respectively), and so treatment with ganciclovir was initiated. NK cell degranulation (as assessed by CD107a expression) was in the normal range. Perforin expression was in the lower normal range, and genetic tests subsequently revealed a heterozygous p.Ala91Val variant. This mutation was not considered relevant because it is common in the general population and was also detected in the healthy father. Due to severe circulatory failure that was refractory to conventional therapy, venous-arterial ECMO was initiated. As the patient's clinical and laboratory profile met the diagnostic criteria for HLH, corticosteroid treatment was initiated on day 2 post-admission. Given the presence of bicytopenia, elevated LDH, and kidney failure, we considered a diagnosis of thrombotic microangiopathy (TMA); however, only a few schistocytes were found in the blood smear. Following an initial improvement in the patient's condition, ECMO was withdrawn after 6 days but this was followed by pulmonary hemorrhage. Brain MRI showed severe hypoxic lesions in all parts of the brain, and an ultrasound assessment of the kidneys revealed hyperechogenic parenchyma. The patient remained anuric, with hemodialysis ruled out by the ongoing pulmonary hemorrhage. Treatment was withdrawn, and the patient died.

P5.2 (P5.1's sister) presented with fever, respiratory distress, and mild thrombocytopenia at the age of 9 months. Laboratory tests revealed anemia (hemoglobin: 68 g/l), thrombocytopenia (14 G/L), leukocytosis (WBC count: 36.7 G/L), elevated ferritin (4800 µg/L), elevated triglycerides (5.5 mmol/L), elevated liver enzymes, low factor V (42%; normal range >60%), and normal albumin and ammonium levels. A CSF analysis gave normal values for protein, glucose, and the cell count. Sapovirus, enterovirus and rhinovirus were detected in the nasopharyngeal aspirate, and HHV6 was the only detected virus by virome analysis (see material and methods) in the patient's blood; treatment with ganciclovir was therefore initiated. Overall, the patient's clinical and laboratory profiles met the diagnostic criteria for HLH, and treatment (dexamethasone, etoposide and cyclosporine) was initiated in line with the HLH2004 protocol. NK cell degranulation (as assessed by CD107a expression) was in the normal range. Perforin expression was abnormally low, and genetic tests subsequently revealed a heterozygous p.Ala91Val variant (as in the patient's brother). A liver biopsy showed hepatocellular necrosis. Bleeding and hemorrhagic shock developed after the liver biopsy, so the patient was transferred to a pediatric intensive care unit at a university medical center.

Kidney failure with anuria occurred on day 5 after the patient's initial presentation, and was treated with dialysis. Cyclosporine treatment was withdrawn, since the drug's possible causal role in kidney failure could not be ruled out. Laboratory tests highlighted the presence of schistocytes. No haptoglobin was detected. The plasma complement SC5b9 level was elevated (671 ng/ml), whereas levels of C3c, C4, ADAMST13, and factors H, B, and I were within the normal range. No anti-factor H antibodies were detected. A kidney biopsy (performed one month after the initial presentation) revealed TMA, and so treatment with anti-complement C5 antibody (eculizumab) was initiated. A kidney biopsy led to bleeding and hemorrhagic shock. During continued treatment with etoposide and lower doses of dexamethasone, a second HLH flare occurred one month after the initial presentation. The flare had probably been triggered by a bacterial infection (*S. epidermidis*), which led to sepsis in the context of etoposide-induced neutropenia. Treatment with anti-thymocyte globulin was initiated, and partial remission of the HLH was achieved. In order to prevent further HLH episodes, treatment with the JAK1/JAK2 inhibitor ruxolitinib was initiated. Two months after the patient's initial presentation, gastrointestinal bleeding was observed. Endoscopy evidenced a large number of small ulcers in the duodenum and throughout the colon. The histopathologic assessment was not conclusive. The dose of dexamethasone was progressively reduced, and the drug was eventually withdrawn in view of the gastrointestinal TMA and possible steroid-induced gastrointestinal bleeding. Treatment with eculizumab and ruxolitinib was maintained.

Three months after the initial presentation, the patient developed tachypnea (initially due to hydrothorax during peritoneal dialysis) requiring oxygen therapy. Despite the resolution of hydrothorax and the absence of any signs of infection, the patient continued to require oxygen.

In the following months, the patient experienced repeated episodes of fever and developed signs of subclinical HLH. Given the lack of a known etiology and therefore the uncertain prognosis for kidney transplantation, combination of the latter with HSCT was not considered to be a viable option. Peritoneal dialysis was initiated, and the patient was discharged to home (almost 5 months after the initial presentation) with oxygen therapy. Two weeks after discharge, the patient presented with respiratory distress and mechanical ventilation was initiated. Pulmonary hemorrhage was diagnosed, and she succumbed to her illness at the age of 16 months.

Kindred 6. The male patient **P6.1** was born to consanguineous parents of Egyptian origin. At the age of 48 months, P6.1 presented with nephrotic nephritic syndrome (heavy proteinuria, elevated creatinine, and hematuria). The patient did not respond to steroid treatment or various immunosuppressants (cyclophosphamide, cyclosporine, and mycophenolate mofetil). At the age of 6 years, a kidney biopsy showed features of membranoproliferative glomerulonephritis. Out of the 15 glomeruli per section, one was sclerotic, four showed mesangial hypercellularity with increased mesangial matrix, and 4 were segmentally sclerotic. The remaining glomeruli and the non-sclerotic elements showed a thickening of the basement membrane. A few atrophic tubules were detected but there was no interstitial fibrosis. The blood vessels were unremarkable. The only extrarenal sign or symptoms were hepatosplenomegaly, anemia and low platelets. The frequency of infections during childhood was reportedly normal. At the age of 9 years (while on mycophenolate

mofetil), P6.1 developed severe sepsis with an unknown focus. The sepsis did not respond to triple antibiotic therapy and progressed to ARDS and death.

Kindred 7. P7.1 was born to consanguineous parents of Native American descent. Her first major episode of illness occurred at 5 months old, with fever, extremity rash, anorexia, lethargy, and rapidly progressive respiratory failure. She was found to have pneumonia on a chest X-ray, and a blood culture was positive for group A *Streptococcus*. The patient had leukocytosis (WBC count: 50 x G/L), thrombocytopenia (42 G/L), anemia, elevated liver enzymes (both ASAT and ALAT: 9000 U/L), hyperferritinemia (12000 µg/L), rhabdomyolysis, splenomegaly, acute kidney injury, ARDS, and low B-cell and NK cell counts. Her condition was diagnosed as toxic shock syndrome with sepsis and multi-organ failure, from which she had recovered completely after 3 weeks.

The patient was in good health between 6 and 11 months of age, with slightly delayed but steady developmental gains. However, at 12 months of age, she presented with fever, cough, and rhinorrhea after having received the diphtheria/tetanus/pertussis/polio/Haemophilus influenzae type b, measles/mumps/rubella and meningitis C vaccines. Over the following week, she developed respiratory failure with leukocytosis (WBC count >50 x 10^9/L), anemia (hemoglobin: 75 g/L), thrombocytopenia (20 G/L), elevated transaminases (ASAT: 281 U/L, ALAT: 108 U/L), hyperferritinemia (2300 µg/L) and elevated C-reactive protein (70 mg/L). She was admitted to the intensive care unit, with multi-organ dysfunction characterized by ARDS, bicytopenia, elevated transaminases, hepatomegaly, splenomegaly, rhabdomyolysis, and rash. An extensive work-up for infectious diseases detected vaccine strain measles virus (in a PCR test of a nasopharyngeal aspirate), anti-measles virus IgM, and Epstein-Barr virus (EBV, PCR blood test: 6.6 x 10^2 copies/mL). A bone marrow aspirate showed hypercellularity and a few hemophagocytes. A liver biopsy revealed non-specific inflammation, and the liver tissue stained negative for EBV, CMV, and herpes simplex virus. The patient was treated with ribavirin, vitamin A, methylprednisone, and a single bolus of intravenous immunoglobulins (IVIG). She left the intensive care unit after six weeks.

At 33 months of age, the patient presented with severe ARDS, bicytopenia, leukocytosis, elevated transaminases, hyperferritinemia (2546 µg/L), splenomegaly, acute kidney injury, and a new, profound, neurologic injury with seizure activity. Brain MRI showed extensive, symmetric, restricted diffusion involving both cerebral hemispheres and the cerebellum, together with dural enhancement. The patient tested positive for influenza B and for *Staphylococcus aureus* in an endotracheal tube culture. She was treated with oseltamivir and antibiotics. She received high-dose IVIG and (due to suspected HLH) high-dose dexamethasone. HSCT was considered but not pursued because of the patient's severe neurologic impairments. At present the patient is alive and being treated with an antiepileptic and a monthly dose of IVIG.

Kindred 8. P8.1 was born to consanguineous parents of Turkish descent. At the age of 2 months, the girl developed severe CMV infection with hepatic disease, lung disease and inflammatory changes in the brain stem. Notably, there was no evidence of retinal disease or hearing loss. The infection had presumably been transmitted through the CMV +ve breast milk,

as CMV DNA was absent in a dried blood spot from the perinatal card. She was treated with ganciclovir and oral valganciclovir throughout the 1st year of life. CMV was never again detected in the subsequent course neither in plasma nor tissue biopsies (brain, liver, lung), while CMV antibodies of IgG isotype remained at unusually high levels. The affected organs, however, did not recover. Nodular changes occurred in the liver as evidenced by ultrasound and liver enzymes never returned to normal levels. Lung imaging showed persistent interstitial lung disease beginning in the first year of life and multiple subpleural cysts consistent with lung fibrosis. While she had chronic dry cough throughout her life, she never required oxygen supplementation. Multiple inflammatory and calcifying lesions developed in the brain. From birth, she showed poor development with failure to thrive, small stature and mental retardation.

At 4 years, the patient presented with nephritic nephrotic kidney disease due to thrombotic microangiopathy, moderately responding to steroids. From the age of 5 years on, the patient has been suffering from chronic recurrent arthritis of the knees with joint effusions and from erythema nodosum. She received regular prednisolone pulse therapy. With progressive vasculitis at multiple organ sites, addition of methotrexate, maintenance steroids, mycophenolate mofetil and everolimus could not prevent a continuous deterioration that led to profound pancytopenia, highly active inflammation and vasculitis (ferritin above 6,000 µg/l, von Willebrand antigen above 300%). HLH criteria (6/8) were fulfilled. With seizures, cerebral palsy and pulmonary hemorrhage requiring artificial ventilation, however, treatment was changed to palliative care. At age 8 years, she succumbed to her relentless disease.

P8.2 (P8.1's brother) was diagnosed with a unilateral double-kidney with megaureter and urinary transport dysfunction II-III° on both sides. Also a congenital heart defect was discovered (haemodynamic irrelevant ASD II). During routine check-up in the second month of life, elevated transaminases, anemia and thrombocytopenia (both requiring transfusions), elevated inflammatory parameters (in the absence of fever), and failure to thrive were noted. Clinical improvement was achieved with pulse IV methylprednisolone and IL-1 blocking (anakinra) therapy. Nevertheless, interstitial lung disease developed requiring O2 supplementation for a total of 4 month.

The patient was in good health between 6 and 15 months of age. However, at 15 months of age, he presented with severe varicella after having received the varicella vaccine.

In the second year of life, an influenza A infection led to hospitalization and he required a prolonged course of oxygen supplementation. Neurologically a severe developmental delay was diagnosed, accompanied by autism spectrum disorder, which is treated with risperidone. At the age of 6,3 years, a second influenza A infection occurred and the patient was admitted to the intensive care unit, with respiratory insufficiency. A prolonged course of high-flow oxygen supplementation was needed. Due to HLH-like multisystem inflammatory disease with need of erythrocyte transfusion, another course of pulse IV methylprednisolone therapy was initiated and led to improvement.

Currently, at age 7,5, the patient is alive and well without any medication but risperidone. A mediastinal lymphadenopathy is currently under investigations concerning mycobacteria (skin test highly positive, IGRA negative).

4. SUPPLEMENTARY TABLES

Supplementary Table 1. Details on inflammatory episodes and organ involvement in patients with ZNFX1-deficiency and affected siblings

ID	Gender	Age	Infectious agent	Hematopoietic	Liver disease	Neurology	Kidney disease	Lung disease	Other	Immunosuppression	Transplant	Outcome
P1.1	F	At birth:	unknown	NA	hepatitis	No	No	No	Failure to thrive (since birth)	NA	No	NA
		6 mo:	unknown	Anemia, lymphadenopathy	hepatomegaly	No	No	Recurrent pneumonia		NA	No	Dead (2y 8mo)
P1.2*	F	6 mo:	unknown	No	elevated liver enzymes	seizures		severe chronic lung disease				
		9 mo:	tuberculin conversion	No								
		1y 6mo:	None	splenomegaly	hepatomegaly							
		3 y:	None					cholesterol pneumonitis	polyarthritis	Steroids, MTX, Aza**		
		7 y:	Influenza A					Pneumonia, restricitve lung function				
		10-15 y:	RSV, Adenovirus			white matter changes (11y), multiple focal calcifications (14y)	Glomerulosclerosis, tubular atrophy, interstitial fibrosis (autopsy)				Lung (10y)	Dead (15y)
P1.3	M	Birth-2 mo:	None	low plts (2 mo)	jaundice (at birth)	multiple focal calcifications (2 mo)			tetralogy of Fallot, failure to thrive (since birth)			
		5 mo	RTI, germ unknown	splenomegaly	hepatomegaly			Interstitial lung disease		Steroids, Aza		
		6 mo	Rota- and Norovirus	HLH	hepatomegaly, elevated liver enzymes, coagulopathy				Intestinal invagination			
		1y 1mo	Influenza A	No		seizures		ARDS				Dead (1y 2mo)
P2.1	F	4 y:	unknown	(Anemia, low plts during TMA, 4)		No	aHUS, TMA	pneumonia	gastroenteritis			
		9-14 y:			Elevated liver enzymes, nodular regenerative hyperplasia (9)							Alive (14)
P2.2	M	At birth:				Microcephaly (since birth)						
		2 mo:	RSV, Rotavirus vaccine (?)	Anemia, low plts	Elevated liver enzymes			Bronchitis				
		2.5 mo:	RSV	Anemia, low plts	Elevated liver enzymes			Bronchitis	Hypothyroidism			
		3 mo:	Influenza A	HLH-like	Acute liver failure, hepatomegaly		Kidney failure during MOF	ARDS				Dead (3 mo)
P3.1	F	Birth-5 mo:	NA	Low plts	NA	Seizures (NA)	NA	NA		NA	No	Dead (5 mo)
P3.2	M	10 mo:	RTI, germ unknown	HLH-like	Elevated liver enzymes	No	No	No	No	No	No	
		11 mo:	Norovirus	HLH-like	Elevated liver enzymes, hepatomegaly	No	No	No	No	No	No	
		1 y:	HHV6	HLH-like	Acute liver failure	Hepatic encephalopathy, seizures, leptomeningeal enhancement, necrotizing encephalopathy	Kidney failure during MOF	ARDS, pulmonary hemorrhage	No	No	No	Dead (1 y)
P4.1	F	7-8 mo:	ADV (7 mo)	HLH (7 mo)	Elevated liver enzymes, hepatomegaly (7 mo)	Seizures, leptomeningeal enhancement, ischemic lesions (7 mo)	Kidney failure during MOF (8 mo)	ARDS, pulmonary hemorrhage (8 mo)		Steroids, IVIG, VP16, CSA (7 mo)	no	Dead (8 mo)

649 ***(Suppl. Table I continued)***

ID	Gender	Age	Infectious agent	Hematopoietic	Liver disease	Neurology	Kidney disease	Lung disease	Other	Immunosuppression	Transplant	Outcome
P4.2	M	9 mo:	RTI, germ unknown	splenomegaly	hepatomegaly	no	no	no	no	no	no	
		1y 10mo	ADV, Parainfluenza	HLH-like	Hepatomegaly, nodular regenerative hyperplasia	Developmental regression, white matter changes (1.8)	Nephrotic syndrome (1.8)	no	no	Steroids (1.8)		
		1y11mo-8y								HSCT (2y 2mo)		Alive (8)
P5.1	M	2-3 mo:	HHV6 (+CMV) (2 mo)	HLH (2 mo)	Acute liver failure, hepatomegaly (2 mo)	Hypoxic ischemia during MOF (3 mo)	Kidney failure during MOF (3 mo)	ARDS, pulmonary hemorrhage (3 mo)		Steroids, IVIG (2-3 mo)	No	Dead (3 mo)
P5.2	F	9 mo - 1y 4 mo:	HHV6 (+Sapovirus, Rhinovirus)	HLH (9 mo)	Elevated liver enzymes, hepatomegaly, coagulopathy (9 mo)	No	TMA (9 mo)	Suspected Interstitial lung disease (10 mo), pulmonary hemorrhage (1y 4 mo)		Steroids, IVIG, VP16, CSA (9 mo) ATG, Eculizumab,(10 mo) Ruxolitinib (1 y)	No	Dead (1y 4mo)
P6.1	M	Birth-9 y:	No infection suspected	Anemia, low plts, splenomegaly	Hepatomegaly							
		4-6 y:	No infection suspected				Nephrotic syndrome (4 y), MPGN (6 y)			Steroids (4 y), CP, CSA, MMF (NA)	No	
		9 y	Sepsis, germ not identified		NA	NA		ARDS				Dead (9 y)
P7.1	F	5 mo:	GroupA Streptococcus	HLH-like	Elevated liver enzymes, hepatomegaly	No	Acute kidney injury	ARDS				
		1 y:	Vacc strain measles (+EBV)	HLH	Elevated liver enzymes, hepatomegaly	No	No	ARDS, pulmonary hemorrhage		Steroids, IVIG		
		2y 9mo:	Influenza B, S. aureus	HLH-like	Elevated liver enzymes	Seizures, extensive restricted diffusion, ischemic lesions developmental regression	Acute kidney injury	ARDS		Steroids, IVIG (2y 9mo)		Alive (3 y)
P8.1	F	2 mo	CMV		Liver disease: hepatomegaly, elevated enzymes, nodular changes	Disseminated inflammatory lesions, calcifications in white matter, seizures		Interstitial lung disease with fibrosis				
		4 y:				developmental regression	TMA nephritic nephrotic syndrome		Erythema nodosum			
		6-8 y:	Unknown trigger	HLH		Seizures, cerebral palsy		Pulmonary hemorrhage		Steroids, MTX, MMF, everolimus	No	Dead (8 y)
P8.2	M	2 mo:	Unknown trigger	HLH-like	Elevated liver enzymes	severe developmental delay		Oxygen support (2-6 mo)	ASD II Duplex kidney and megaurether	Steroids, anakinra		
		1y 3mo:	Vacc strain VZV	Severe varicella (not further specified	NA	NA	NA	NA		NA		
		2 y:	Influenza A			Autism sspectrum disorder		Prolonged oxygen support				
		6 y:	Influenza A	HLH-like				Prolonged oxygen support		Steroids		Alive (7 y)
Summary		female to male: 8:7	Number of severe viral infections by (-)ssRNA viruses: 10 (+)ssRNA viruses: 2 dsRNA viruses: 1 dsDNA viruses: 7	Episodes triggered by infections: HLH: 6 HLH-like: 9 ARDS: 8	Neurological involvement in n= 11 patients		Nephrological involvement in n=11 patients	Pulmonary involvement in n= 13 patients		Limited success with immunosuppressive therapy HSCT arrested disease in n=1		Alive:dead: 4:11

Table S1: Clinical phenotypes. In bold: virally triggered disease. Numbers in brackets denote age in years. ADV: adenovirus; ATG: anti-thymoglobulin; CSA: cyclosporine A; (CMV): low copy number of cytomegalovirus in blood by PCR; CP: cyclophosphamide; (EBV): low copy number of Epstein Barr virus in blood by PCR; HLH: hemophagocytic lymphohistiocytosis; HHV6: human herpesvirus type 6; HSCT: hematopoietic stem cell transplant; Infl: influenza; IVIG: intravenous immunoglobulins; MMF: mycophenolate mofetil; MTX: methotrexate; NA: information not available; Parainfl: human parainfluenza virus; RTI: respiratory tract infection; VP16: etoposide;

*Treatment: only immunosuppressive and immunomodulatory treatments before transplants are indicated here

**For P1.2: infections after lung transplant are not mentioned in this table.

Supplementary Table 2: Live vaccine side effects

Patient ID	Live vaccine (age)	Temporarily associated clinical problems	Side effect after live vaccine: relationship between clinical problem and live vaccine		
			None	Unlikely	Definitely
P1.1	NA				
P1.2	MMR (1)	None	X		
P1.3	NA				
P2.1	MMR VZV (1)	None	X		
P2.2	Rotavirus (0.2)	RSV and Influenza A infection, liver failure, ARDS, death (0.3)		X	
P3.1	None				
P3.2	MMR (1)	HHV6, HLH-like disease, multi-organ failure (1)		X	
P4.1	NA				
P4.2	NA				
P5.1	None				
P5.2	None				
P6.1	BCG (0.2) MMR (1.3) OPV (0.2; 0.3; 0.5; 1.5)	None	X		
P7.1	MMR (1)	Vaccine strain measles and low-level EBV viremia, HLH and ARDS			X
P8.1	MMR (1)		X		
P8.2	MMR VZV (1.3)	Vaccine strain varicella			X

Table S2: Live-attenuated vaccines and adverse reactions. Only temporally associated clinical events are listed (<1 month after live vaccine administration). None: no clinical events during the month following live vaccine; unlikely: although temporally associated clinical events, other cause possible; Definitely: temporal relationship, no other cause evident, detection of vaccine strain in body fluids or organ tissue (measles) or typical rash (VZV); ARDS: acute respiratory distress syndrome; HHV6: human herpesvirus type 6; HLH: hemophagcytic lymphohistiocytosis; MMR: measles, mumps, and rubella; RSV: respiratory syncythial virus; VZV: varicella zoster virus.

Supplementary Table 3: Diagnostic Criteria for Pediatric Acute Liver Failure

Patient ID	Hepatomegaly	ASAT (UI/L, max.)	ALAT (UI/L, max.)	Coagulopathy	INR (max.)	Bilirubin total (umol/L, max.)	Bilirubin conjugated (umol/L, max.)	GGT (U/L, max.)	Albumin (g/L, min.)	LDH (UI/L, max.)	Hepatic encephalopathy	PALF criteria fulfilled:
P1.1	Yes	elevated	elevated	NA	NA	NA	NA	NA	NA	NA	No	unknown
P1.2	Yes	118	151	No	1.2	6.8	NA	302	34	1626	No	No
P1.3	Yes	3184	918	Yes	1.4	17.1	NA	566	15.6	4674	No	No
P2.1	No	elevated	elevated	NA	NA	NA	NA	NA	NA	increased (age 4 y)	No	unknown
P2.2	Yes	10521	2472	Yes	2.7	159.0	97	49	22.8	17735	No	Yes
P3.1	NA	NA	NA	NA	NA	NA	NA	NA	NA	NA	NA	unknown
P3.2	Yes	10217	2420	Yes	1.5	41.0	24	117	18	11476	Yes	Yes
P4.1	Yes	2910	751	NA	NA	NA	NA	NA	NA	NA	No	unknown
P4.2	Yes	83	64	NA	NA	NA	NA	NA	NA	NA	NA	unknown
P5.1	Yes	13375	2350	Yes	2.9	77.0	48	146	17	9209	possible	Yes
P5.2	Yes	161	253	Yes	1.2	19.0	5	352	33	2499	No	No
P6.1	Yes	elevated	elevated	NA	NA	NA	NA	NA	18	NA	NA	unknown
P7.1	Yes	9000s	9000s	No	1.2	12.0	7	423	15	1569	No	No
P8.1	Yes	400	629	Yes	1.5	16.0	NA	800	28	1065	No	No
P8.2	Yes	482	280	Yes	1.4	9.0	NA	228	NA	1355	No	No

Table S3: Diagnostic criteria for Pediatric acute liver failure, according to the criteria of the PALF study group (Squires et al.)(1); NA: not available; PALF: Pediatric acute liver failure; y: years; ASAT: Aspartate transaminase; ALAT: Alanine transaminase; INR: International normalized ratio; GCT: Gamma-glutamyl transferase; PALF: Pediatric acute liver failure.

Supplementary Table 4: Demographic and Genetic Characteristics of Patients

Pat. ID	Gender	Consanguinity	Ethnic Origin / country of origin	Genomic Location Chr20 (GRCh37)	Variant cDNA (NM_021035.2)	Amino acid change (NP_066363.1)	Exon number	Impact	CADD Score (phred)	PROVEAN Score	Polyphen-2 Score	SIFT Score	gnomAD allele frequency	VarCards D:A Score	VarCards Extreme	Functional Domain
P1.1	F	Yes	Arabian	NA	NA	NA	NA	NA	NA	NA	NA	NA	NA	NA	NA	NA
P1.2	F	Yes	Arabian	g.[47887853T>TA]; [47887853T>TA]	c.[495_496insT]; [495_496insT]	p.(Thr166TyrfsTer17); (Thr166TyrfsTer17)	3 / 14	Frameshift/ Framshift	25.4 / 25.4	- / -	- / -	- / -	Absent / Absent	- / -	- / -	ARM repeat
P1.3	M	Yes	Arabian	g.[47887853T>TA]; [47887853T>TA]	c.[495_496insT]; [495_496insT]	p.(Thr166TyrfsTer17); (Thr166TyrfsTer17)	3 / 14	Frameshift/ Framshift	25.4 / 25.4	- / -	- / -	- / -	Absent / Absent	- / -	- / -	ARM repeat
P2.1	F	No	Europe	g.[47872450C>CA]; [47886725TGA>T]	c.[2698_2699insT]; [1623_1624delTC]	p.(Arg900MetfsTer5); (His542CysfsTer41)	9 / 14	Frameshift/ Frameshift	28.8 / 24.1	- / -	- / -	- / -	Absent / Absent	- / -	- / -	P-loop containing nucleoside triphosphate hydrolase / ARM repeat
P2.2	M	No	Europe	g.[47872450C>CA]; [47886725TGA>T]	c.[2698_2699insT]; [1623_1624delTC]	p.(Arg900MetfsTer5); (His542CysfsTer41)	9 / 14	Frameshift/ Frameshift	28.8 / 24.1	- / -	- / -	- / -	Absent / Absent	- / -	- / -	P-loop containing nucleoside triphosphate hydrolase / ARM repeat
P3.1	F	Yes	Syria	NA	NA	NA	NA	NA	NA	NA	NA	NA	NA	NA	NA	NA
P3.2	M	Yes	Syria	g.[47887952T>A]; [47887952T>A]	c.[397A>T]; [397A>T]	p.(Lys133Ter); (Lys133Ter)	9 / 14	Nonsense/ Nonsense	34 / 34	- / -	- / -	- / -	Absent / Absent	10:12 / 10:12	Yes / Yes	- / -
P4.1	F	No	Europe	g.[47866100A>G]; [47865686C>G]	c.[3461T>C]; [3875G>C]	p.(Ile1154Thr); (Cys1292Ser)	14 / 14	Missense/ Missense	25.1 / 25.4	-4.48 / - 9.33	PD/ PD	D/D	Absent / Absent	23:23 / 23:23	Yes / Yes	P-loop containing nucleoside triphosphate hydrolase
P4.2	M	No	Europe	g.[47866100A>G]; [47865686C>G]	c.[3461T>C]; [3875G>C]	p.(Ile1154Thr); (Cys1292Ser)	14 / 14	Missense/ Missense	25.1 / 25.4	-4.48 / - 9.33	PD/ PD	D/D	Absent / Absent	23:23 / 23:23	Yes / Yes	P-loop containing nucleoside triphosphate hydrolase
P5.1	M	No	Turkey	g.[47865770C>G]; [478684378TTCTC>T]	c[3791G>C] [5179_5183delGAG AA]	p.(Cys1264Ser); (Glu1727LysfsTer11)	14 / 14	Missense/ FrameShift	29.3 / -	-9.36 / -	D / -	D / -	Absent / 1.22e-05	23:23 / -	Yes / -	- / -
P5.2	F	No	Turkey	g.[47865770C>G]; [478684378TTCTC>T]	c[3791G>C]; [5179_5183delGAG AA]	p.(Cys1264Ser); (Glu1727LysfsTer11)	14 / 14	Missense/ FrameShift	29.3 / -	-9.36 / -	D / -	D / -	Absent / 1.22e-05	23:23 / -	Yes / -	- / -
P6.1	M	Yes	Egypt	g.[47887219C>T]; [47887219C>T]	c.[1130G>A]; [1130G>A]	p.(Arg377Gln); (Arg377Gln)	3 / 14	Missense/ Missense	27.9 / 27.9	-3.34 / - 3.34	PD/ PD	D/D	Absent / Absent	23:23 / 23:23	Yes / Yes	ARM repeat / ARM repeat
P7.1	F	Yes	Oji-Cree	g.[47887219C>T]; [47887219C>T]	c.[3152T>C]; [3152T>C]	p.(Leu1051Pro); (Leu1051Pro)	12/ 14	Missense/ Missense	34	-6.128 / - 6.128	PD/ PD	D/D	Absent / Absent	22:23 / 22:23	Yes / Yes	P-loop containing nucleoside triphosphate hydrolase
P8.1	F	Yes	Turkey	g.[47887348del]; [47887348del]	c.[1001del]; [1001del]	p.(Arg334Glnfs*67); (Arg334Glnfs*67)	3/ 14	FrameShift / FrameShift	- / -	- / -	- / -	- / -	Absent / Absent	- / -	- / -	ARM repeat / ARM repeat
P8.2	M	Yes	Turkey	g.[47887348del]; [47887348del]	c.[1001del]; [1001del]	p.(Arg334Glnfs*67); (Arg334Glnfs*67)	3/ 14	FrameShift / FrameShift	- / -	- / -	- / -	- / -	Absent / Absent	- / -	- / -	ARM repeat / ARM repeat

Table S4. Demographic and genetic characteristics of patients. All mutations were exonic, CADD: Combined Annotation Dependent Depletion (tool for scoring the deleteriousness of single nucleotide variants as well as insertion/deletions variants in the human genome); Comp. HET: compound heterozygous mutations; D: damaging; F: female; gnomAD: genome Aggregation Database (from an international coalition of investigators with the goal of aggregating and harmonizing both exome and genome sequencing data from a wide variety of large-scale sequencing projects); HOM: homozygous mutations; M: male ; NA: not available; NM: Reference sequence category for mRNA ; NP: Reference sequence category for protein ; PD: probably damaging; Polyphen-2: Polymorphism Phenotyping v2 (tool which predicts possible impact of an amino acid substitution on the structure and function of a human protein); PROVEAN: Protein Variation Effect Analyzer (software tool which predicts whether an amino acid substitution or indel has an impact on the biological function of a protein); SIFT: Sorting Intolerant From Tolerant (score predicts whether an amino acid substitution affects protein function based on sequence homology and the physical properties of amino acids).

5. SUPPLEMENTARY FIGURES

Supplementary Figure 1:

A

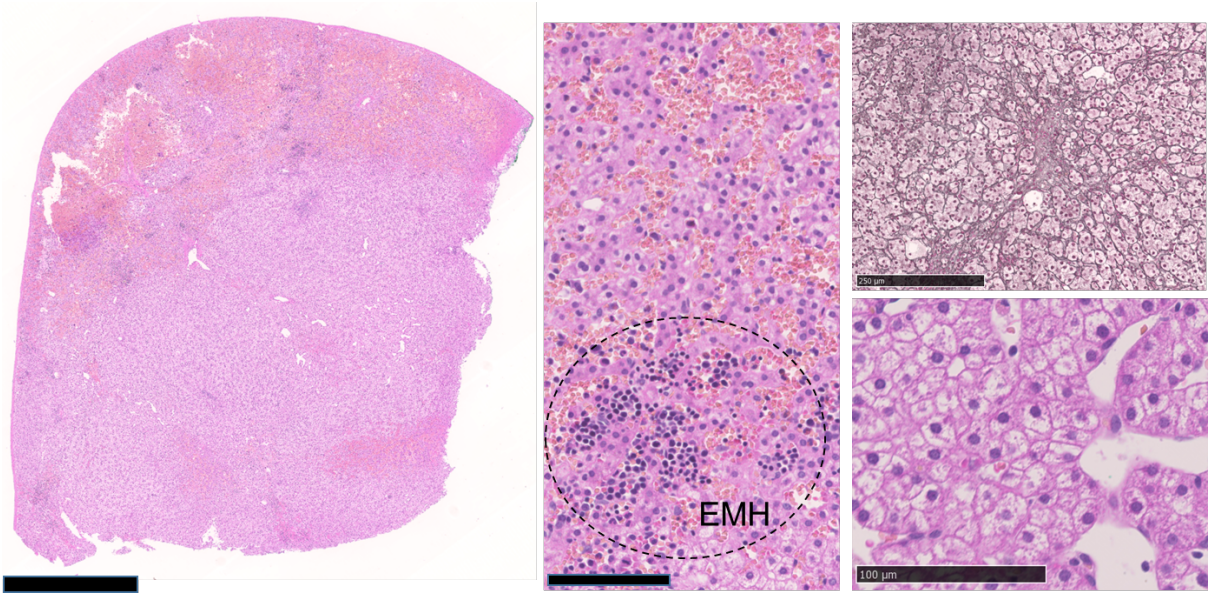

B

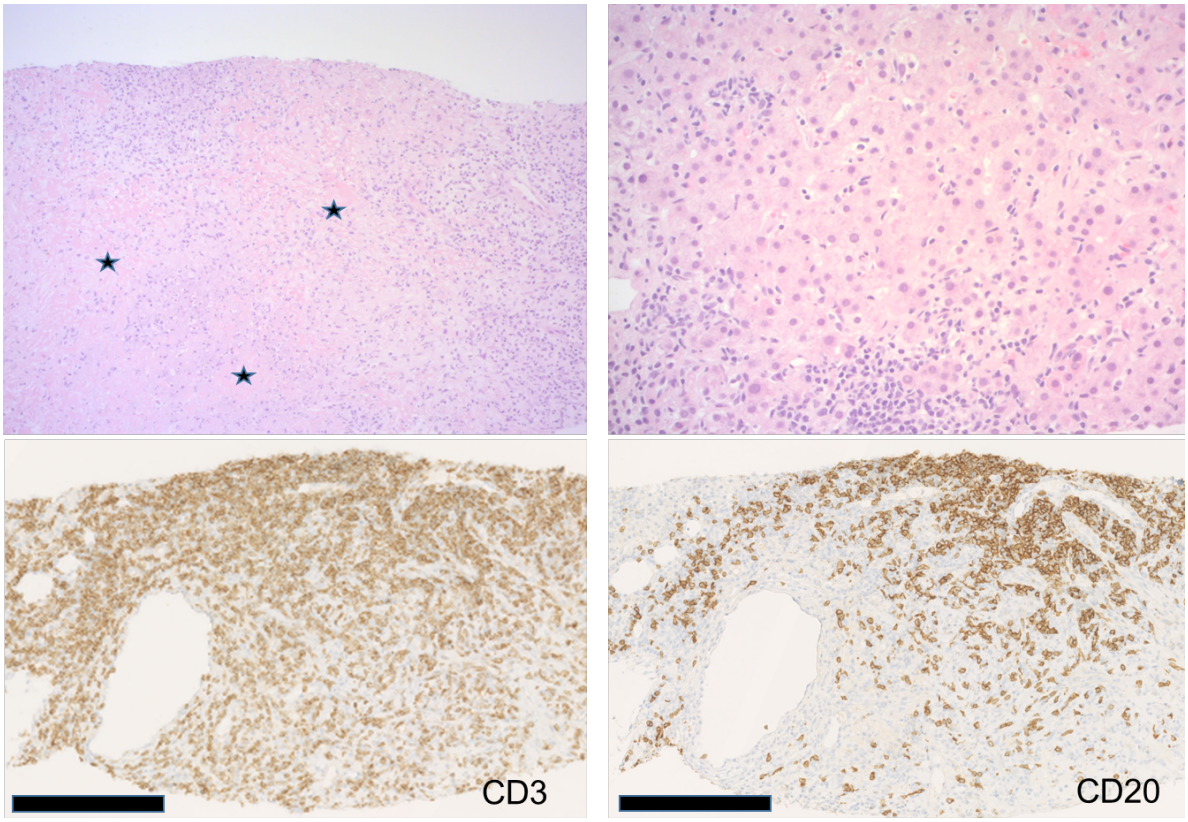

C

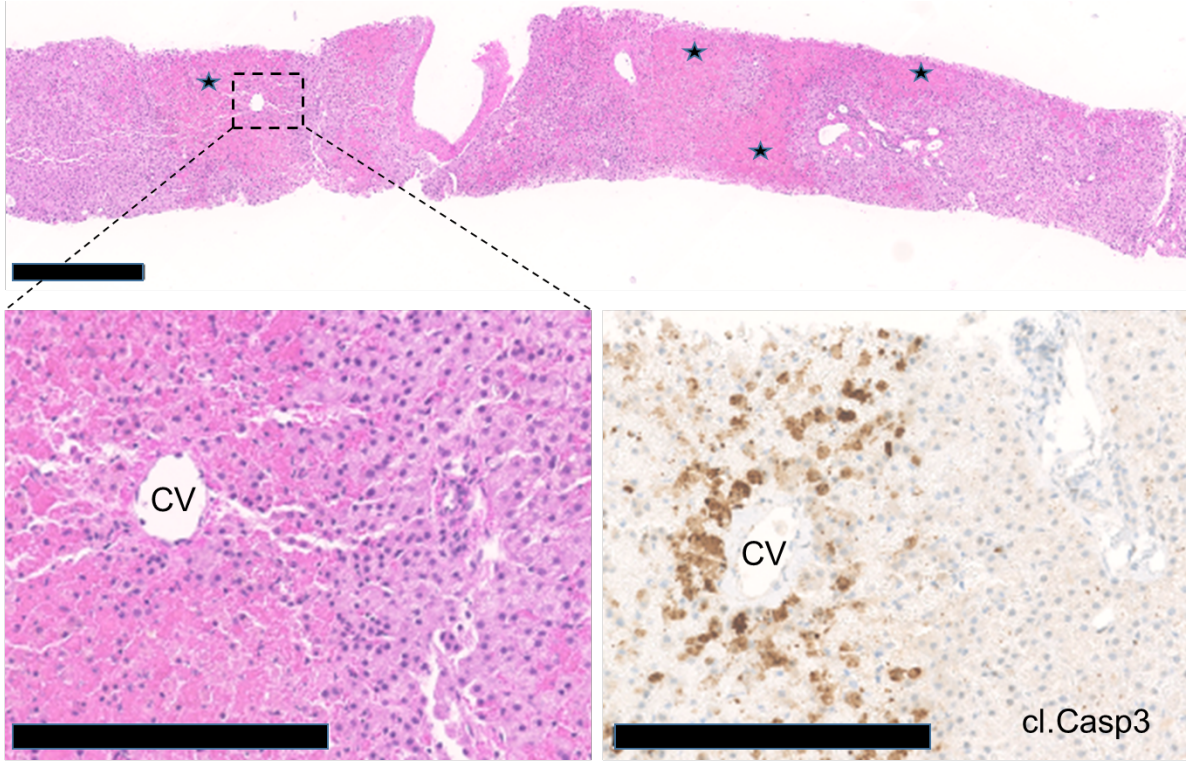

Fig S1: Spectrum of histopathologic changes in the liver. Panel A, Liver biopsy of P1.3. Overview (left) displays subcapsular liver tissue. Detail view (middle) reveals sinusoidal ectasia filled with red blood cells and foci of extramedullary hematopoiesis (EMH), as well as mildly altered architecture with multifocally obliterated sinusoids (upper right, silver reticulin stain), and irregularly arranged plates of hepatocytes with bright cytoplasm (lower right). Scale bars: 500 mm top), 100 mm (lower left), 250 mm (lower right).
Panel B, Liver biopsy of P2.1. Upper panel: Overview (left) displays areas of widespread (panlobular) necrosis (asterisks) with collapse and red cell extravasation. Detail view (right) reveals viable areas with dense immune cell infiltrates rich in lymphocytes and plasma cells. Lower panel: Immunohistochemical analysis confirms a mixed immune cell infiltrate including CD3+ and CD20+ cells. Magnification, upper panel: 10x (left), 20x (right). Scale bars (lower panel): 250 mm.
Panel C, Liver biopsy of P5.2. Upper panel: Overview displays confluent hepatocyte death predominantly in centrilobular areas (asterisks). Lower panel: Detail view reveals hepatocyte death and red blood cell extravasation accentuated around the central veins (CV), sparing periportal areas (right side of image). Hepatocyte cell death highlighted by cleaved Caspase 3 (cl.Casp3) immunohistochemistry (same area, consecutive slide). Scale bars: 500 mm (upper panel), 250 mm (lower panel).

Supplementary Figure 2:

Panel1

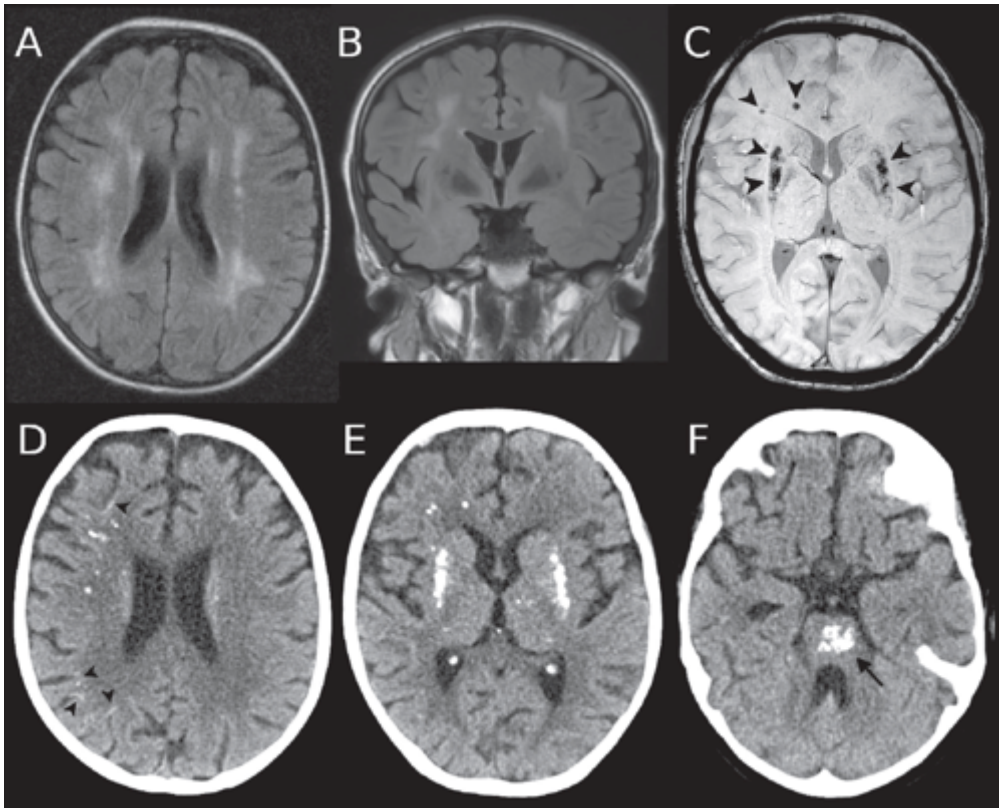

Panel 2

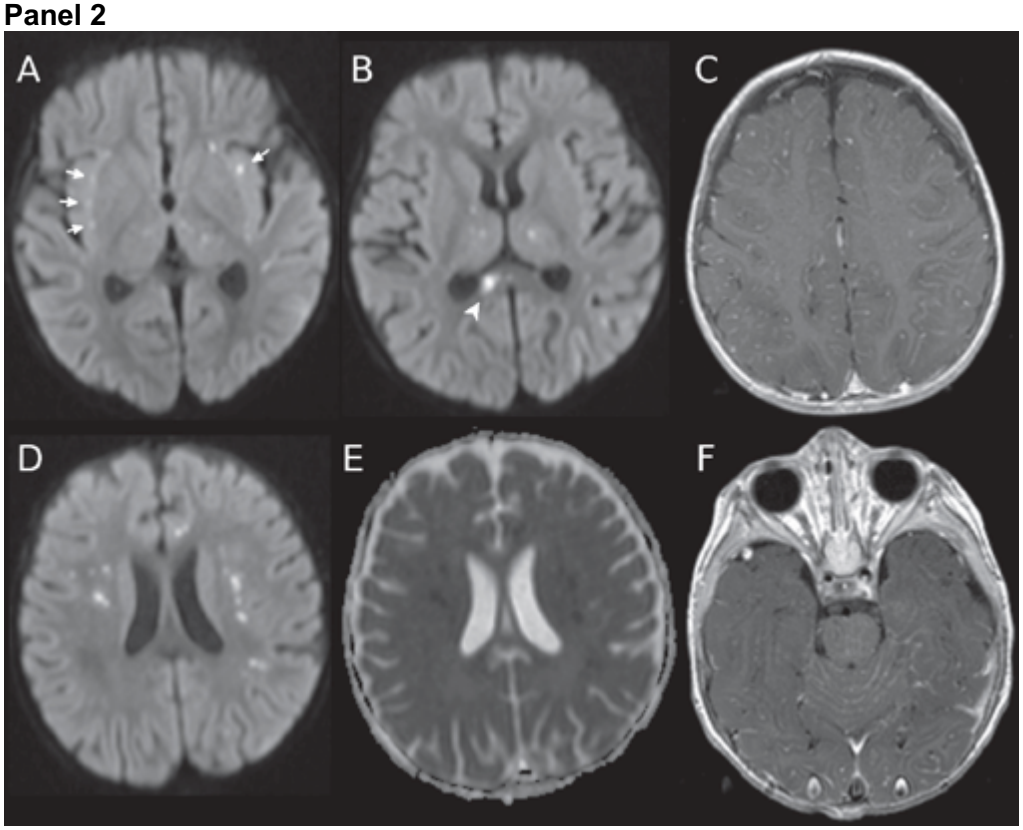

Panel 3

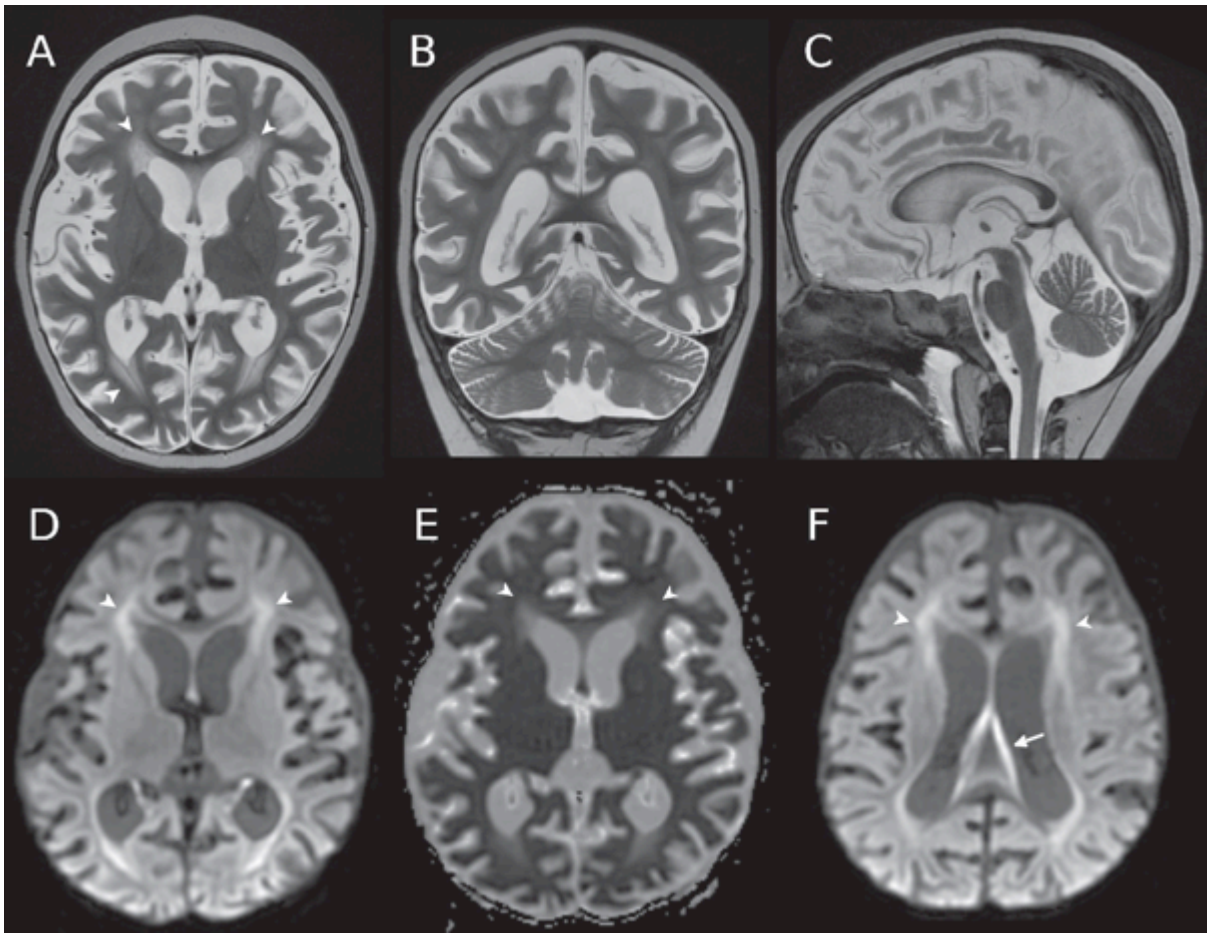

Fig S2: Brain MRI in patients with ZNFX1 deficiency. Panel 1, P1.2. White matter changes on an axial FLAIR image at the age of 11 years (A). The leukoencephalopathy had not progressed at the age of 14 (B). Calcification of the basal ganglia and white matter on susceptibility-weighted imaging at 14 years of age (arrowheads in C). Computed tomography at 15 years of age, showing calcification of the basal ganglia, thalami, white matter, cortex (arrowheads in D), and pons (arrow in F) (D, E, F). Mild atrophy. No cerebellar calcifications. **Panel 2**, P3.2. MRI at the age of 12 months. Multiple acute ischemic lesions on diffusion-weighted imaging, in white matter (A,D,E), splenium (arrowhead in B), thalami (A,B), external capsules and insula (arrows in A) in both hemispheres. Diffuse leptomeningeal enhancement suggestive of HLH on contrast-enhanced T1-weighted images (C, F). **Panel 3**, P5.2, MRI at the age of 13 months. T2-weighted images (A, B, C) and diffusion-weighted images (D,E,F) with an apparent diffusion coefficient map (E). Marked supratentorial atrophy (A, B). Periventricular T2 hyperintensity, which was especially prominent around the anterior and posterior horns of the lateral ventricles (arrowheads in A), with some restricted diffusion (arrowheads in D, E, F). T2 hyperintensity on the undersurface of the corpus callosum (C). T2 hyperintensity in the fornices (body and crura), with intensity on diffusion-weighted images (arrow in F).

Supplementary Figure 3:

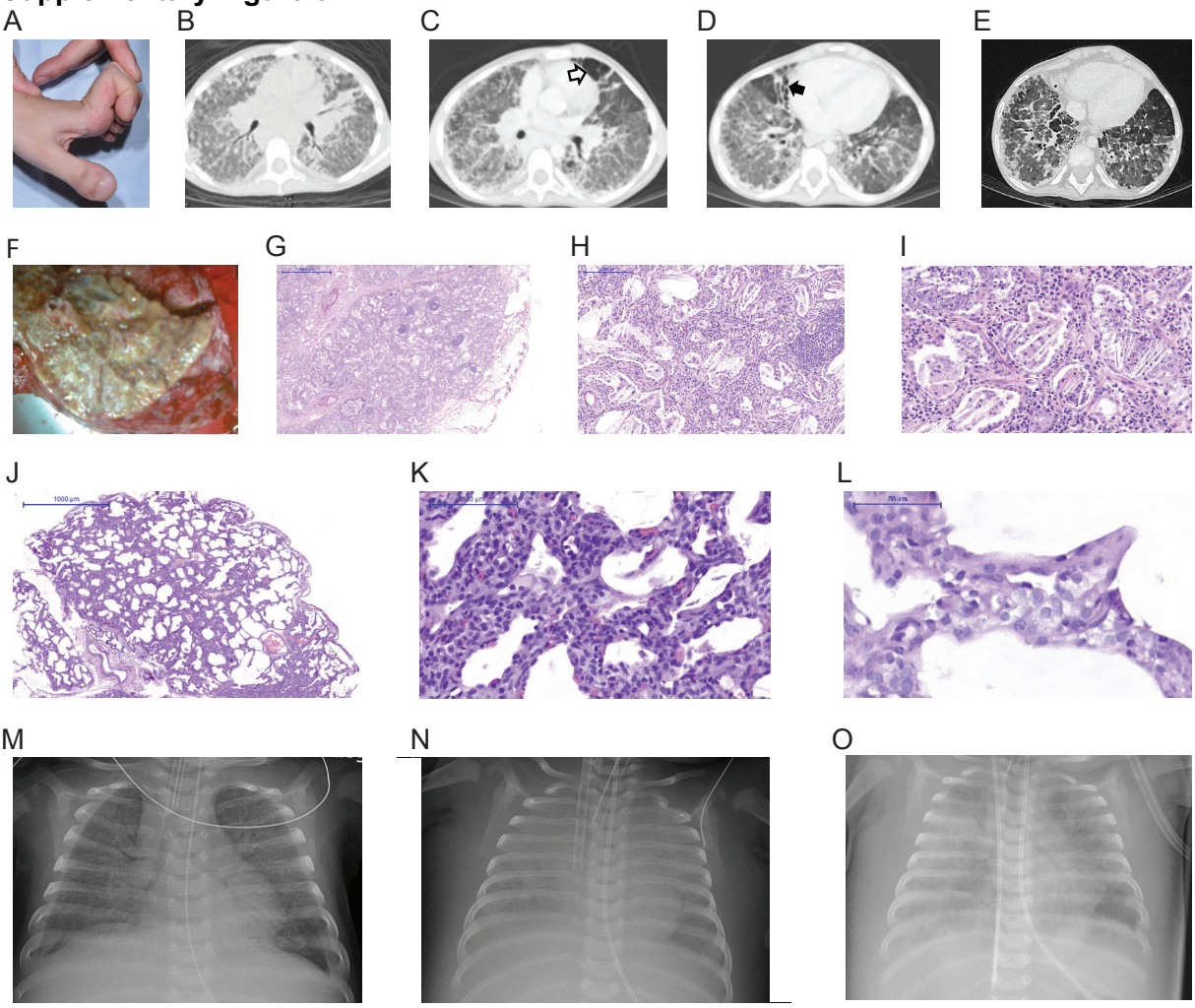

Fig S3: Lung disease caused by ZNFX1 deficiency. Patient P1.2 (**Panel A**) at the age of 10 years, with severe clubbing, joint hypermobility, and chronic joint pain. (**Panel B**) A CT scan at the age of 7 years, showing diffuse ground glass, septal thickening, consolidation, and hilar lymphadenopathy. (**Panels C to E**) At the age of 10 years, we observed more pronounced interseptal thickening, cyst formation (open arrow), and traction bronchiectasis (closed arrow). (**Panel F**) A lung explant was hard and yellow. (**Panels G to I**) Features consistent with cholesterol pneumonitis: (**Panel G**) Overview of the lung tissue with multiple cholesterol granulomas and foam cells in airspaces, with a moderate chronic interstitial inflammatory infiltrate and follicular hyperplasia, hematoxylin and eosin stain (H&E) x20; (**Panel H**) Cholesterol granulomas and foam cells in airspaces. An interstitial inflammatory infiltrate, dominated by lymphocytes and plasma cells, H&E x100; (**Panel I**) Cholesterol granulomas and foam cells in airspaces. An interstitial inflammatory infiltrate, dominated by lymphocytes and plasma cells, H&E x200. Patient P1.3 (**Panel J**) A lung biopsy at the age of 1 year, with irregularly expanded airspaces and widened alveolar septa (H&E x20). (**Panel K**) Hypercellular alveolar septa expanded by mesenchymal cells and resembling pulmonary interstitial glycogenosis. There were few intraalveolar foam cells (arrow), no significant interstitial inflammatory infiltrate, and no cholesterol clefts, H&E x200. (**Panel L**) Oval cells with vacuolated, periodic acid-Schiff (PAS)-negative cytoplasm, PAS x400. Patient P5.1 (**Panel M**) Lung X-ray at presentation (aged 3 months), with fine reticular ground glass opacification. (**Panel N**) 4 days later, the lung was almost completely opaque, and (**Panel O**) another 2 days later (the last X-ray before death) with some air entry on the left side and in the upper lobes. Note the massive edema of the skin.

Supplementary Figure 4:

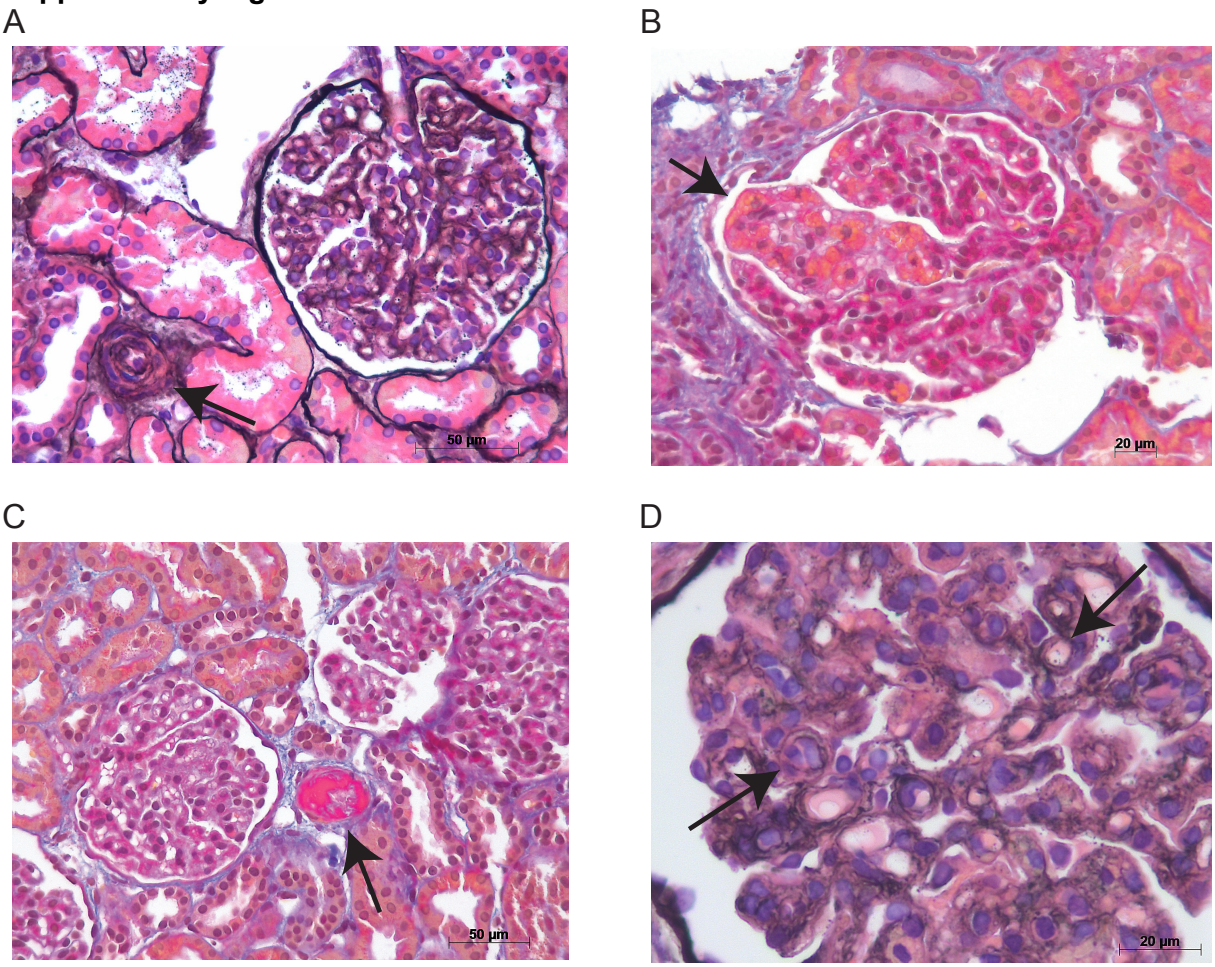

Fig S4: Thrombotic microangiopathy, with acute and chronic lesions. Panel A, thrombosis in a hilar arteriole (arrow). **Panel B**, a glomerulus with prominent segmental mesangiolysis (arrow). **Panel C**, arrow indicating an arteriole with an "onion skin" pattern. **Panel D**, extensive glomerular basement membrane remodeling, with thickening and duplication. Panels A and B: trichrome staining, original magnification 200x for Panel A and 400x for Panel B. Panels C and D: PAS staining, original magnification 200x for Panel C and 640x for Panel D; scale bar: 50 µm (except in panel B: 20 µm).

Supplementary Figure 5:

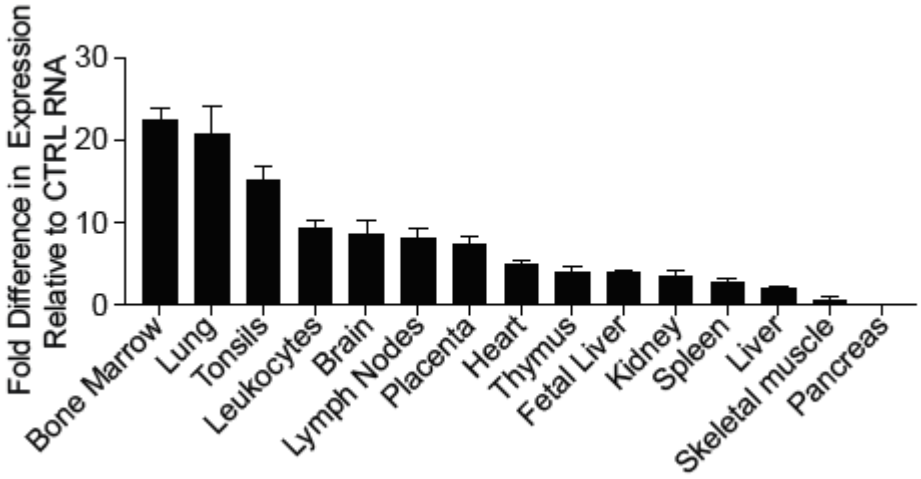

Fig S5: ZNFX1 is ubiquitously expressed but predominantly in the hematopoietic system. Tissue expression of ZNFX1, as detected by a qPCR analysis of organ-specific RNA libraries from multiple donors. The relative ZNFX1 mRNA level in each organ was calculated relative to a control RNA library and standardized against 18S RNA expression. Columns and error bars represent the means and standard deviations of quadruplicate measurements.

Supplementary Figure 6:

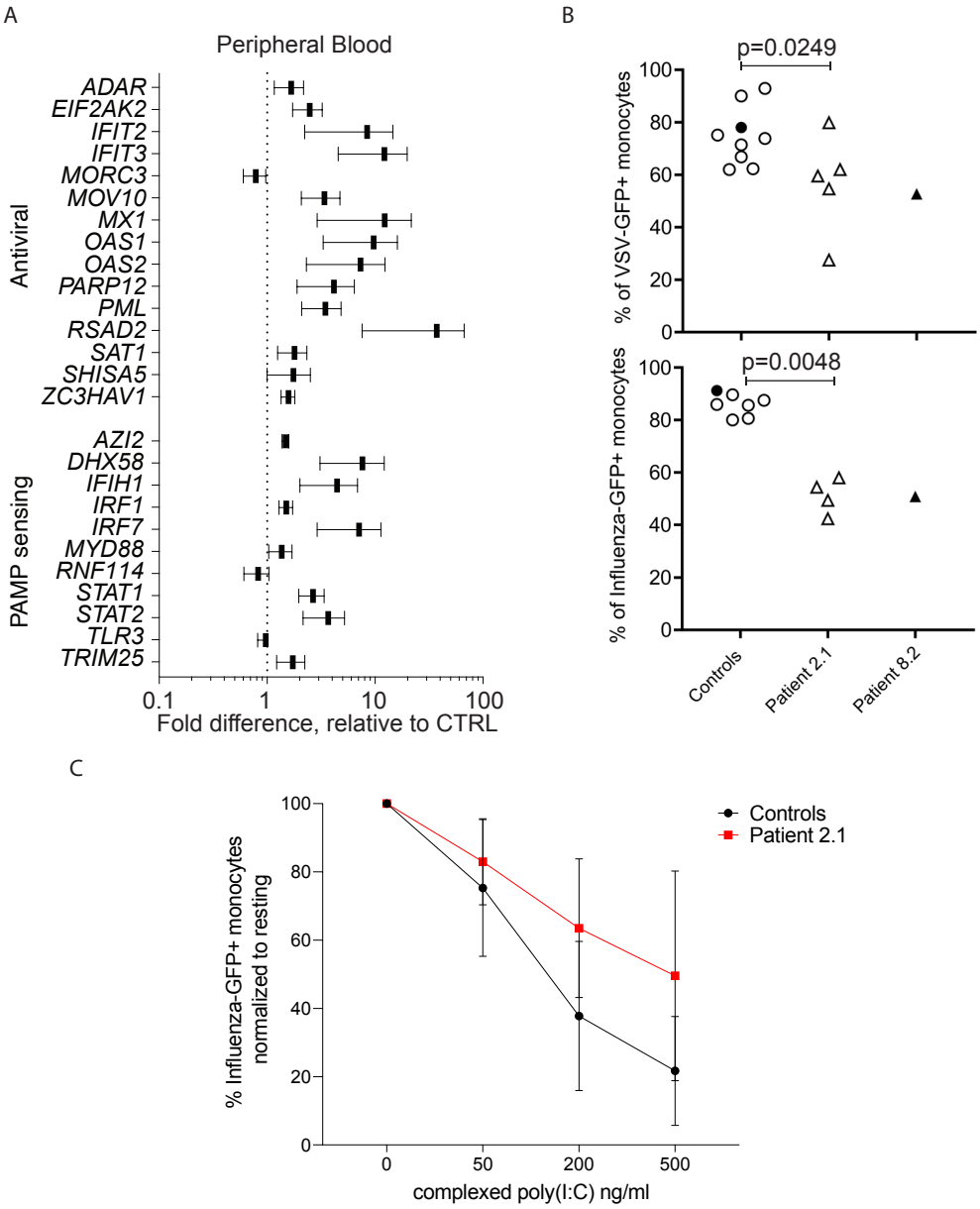

Fig S6: Higher basal ISG expression and lower basal infection rate in ZNFX1 deficiency. Panel A: Transcriptomic analysis of the level of expression of representative ISGs with antiviral and PAMP functions in PBMCs from P1.2 (two samples) and P2.1 (1 samples). Black boxes represent the mean fold difference vs. healthy controls. Error bars show the standard error of the mean for the three samples. **Panel B:** Percentage of VSV-GFP positive monocytes measured by FACS. PBMCs from patient 2.1, 8.2 (triangle symbols) and healthy controls (circle symbols) were infected with VSV-GFP (upper) or Influenza-GFP (lower) for 5 h. One single experiment is shown for patient 8.2 and its respective control (black triangle and black circle symbols). pValues were calculated using Man-Whitney U test, One-tailed. **Panel C:** Flow cytometry analysis of monocytes from Patient 2.1 and healthy control (Controls) pre-treated for 12 hours with different concentrations of lyovec-poly(I:C) and subsequently infected with Influenza-GFP virus. Mean percentage of VSV-GFP positive monocytes relative to the unstimulated condition (no lyovec-poly(I:C)) for four repeats. Error bars refer to ± SD, n=4.

Supplementary Figure 7:

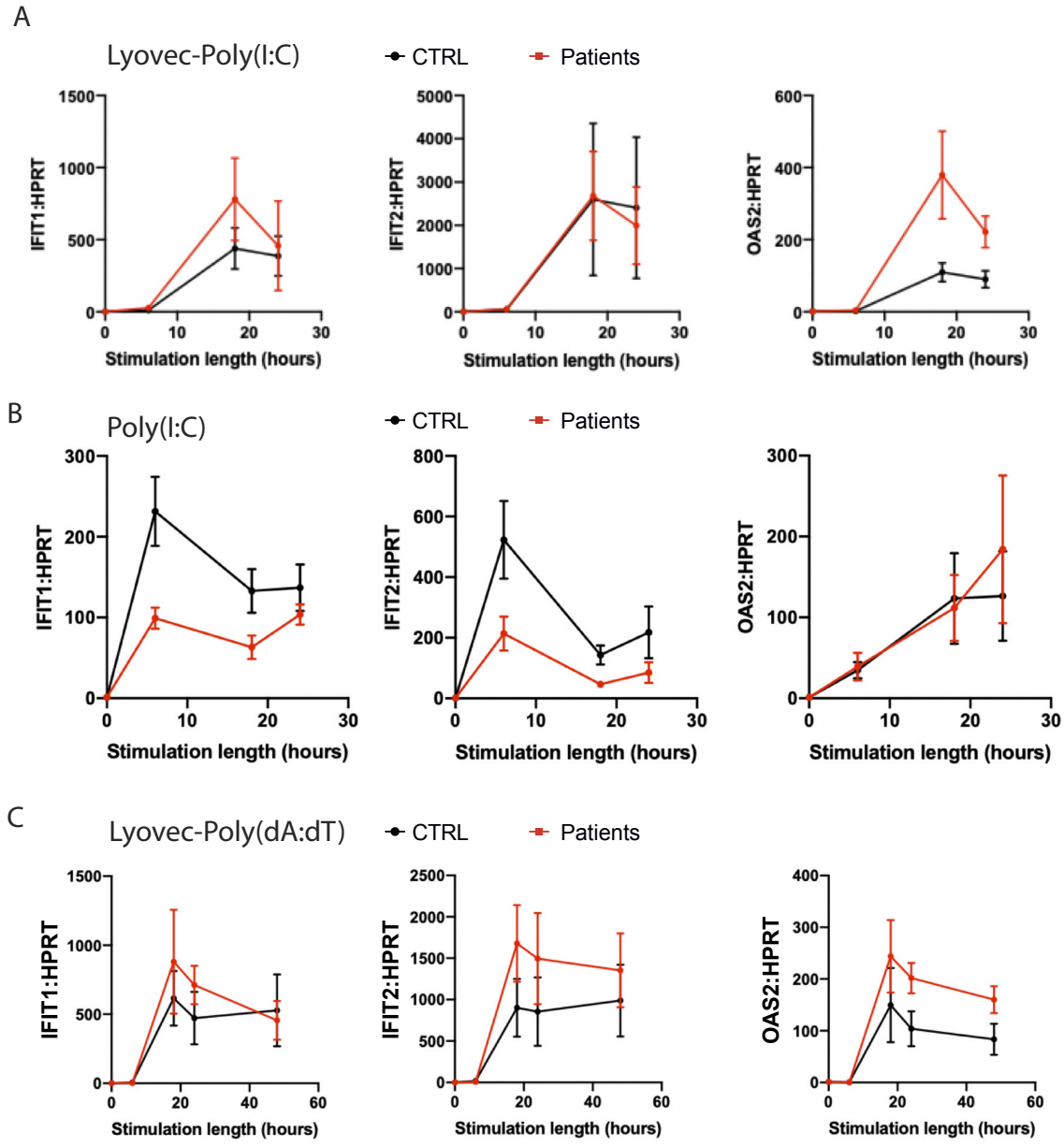

Fig. S7: qPCR of IFIT1, IFIT2 and OAS2 expression, normalized to the housekeeping gene HPRT, in dermal fibroblasts stimulated with transfected poly(I:C) (Lyovec-Poly(I:C)), soluble poly(I:C) (Poly(I:C)) or transfected poly(dA:dT) (Lyovec-Poly(dA:dT) for the indicated times from P1.2, P2.1, P3.2 and P5.2 (Patients, red lines) and four controls (CTRL, black lines). Mean of relative amounts (ΔΔCT) measured in fibroblasts from the 4 patients or 4 controls are expressed relative to the value obtained prior to stimulation (time 0 hours) for each individual. Data are representative of 5 independent experiments. Bars indicate standard error of the mean.

SUPPLEMENTARY REFERENCES

1. Henter JI, Horne A, Arico M, Egeler RM, Filipovich AH, Imashuku S, et al. HLH-2004: Diagnostic and therapeutic guidelines for hemophagocytic lymphohistiocytosis. Pediatr Blood Cancer. 2007;48(2):124-31.
2. Squires RH, Jr., Shneider BL, Bucuvalas J, Alonso E, Sokol RJ, Narkewicz MR, et al. Acute liver failure in children: the first 348 patients in the pediatric acute liver failure study group. J Pediatr. 2006;148(5):652-8.
3. Evans CA, Pinner J, Chan CY, Bowyer L, Mowat D, Buckley MF, et al. Fetal diagnosis of Mowat-Wilson syndrome by whole exome sequencing. Am J Med Genet A. 2019;179(10):2152-7.
4. Paila U, Chapman BA, Kirchner R, Quinlan AR. GEMINI: integrative exploration of genetic variation and genome annotations. PLoS Comput Biol. 2013;9(7):e1003153.
5. Richards S, Aziz N, Bale S, Bick D, Das S, Gastier-Foster J, et al. Standards and guidelines for the interpretation of sequence variants: a joint consensus recommendation of the American College of Medical Genetics and Genomics and the Association for Molecular Pathology. Genet Med. 2015;17(5):405-24.
6. Amendola LM, Jarvik GP, Leo MC, McLaughlin HM, Akkari Y, Amaral MD, et al. Performance of ACMG-AMP Variant-Interpretation Guidelines among Nine Laboratories in the Clinical Sequencing Exploratory Research Consortium. Am J Hum Genet. 2016;99(1):247.
7. Nykamp K, Anderson M, Powers M, Garcia J, Herrera B, Ho YY, et al. Sherloc: a comprehensive refinement of the ACMG-AMP variant classification criteria. Genet Med. 2017;19(10):1105-17.
8. Karbassi I, Maston GA, Love A, DiVincenzo C, Braastad CD, Elzinga CD, et al. A Standardized DNA Variant Scoring System for Pathogenicity Assessments in Mendelian Disorders. Hum Mutat. 2016;37(1):127-34.
9. Thorvaldsdottir H, Robinson JT, Mesirov JP. Integrative Genomics Viewer (IGV): high-performance genomics data visualization and exploration. Brief Bioinform. 2013;14(2):178-92.
10. Sobreira N, Schiettecatte F, Valle D, Hamosh A. GeneMatcher: a matching tool for connecting investigators with an interest in the same gene. Hum Mutat. 2015;36(10):928-30.
11. Marchler-Bauer A, Lu S, Anderson JB, Chitsaz F, Derbyshire MK, DeWeese-Scott C, et al. CDD: a Conserved Domain Database for the functional annotation of proteins. Nucleic Acids Res. 2011;39(Database issue):D225-9.
12. Marchler-Bauer A, Anderson JB, Derbyshire MK, DeWeese-Scott C, Gonzales NR, Gwadz M, et al. CDD: a conserved domain database for interactive domain family analysis. Nucleic Acids Res. 2007;35(Database issue):D237-40.
13. Lu S, Wang J, Chitsaz F, Derbyshire MK, Geer RC, Gonzales NR, et al. CDD/SPARCLE: the conserved domain database in 2020. Nucleic Acids Res. 2020;48(D1):D265-D8.
14. Zimmermann L, Stephens A, Nam SZ, Rau D, Kubler J, Lozajic M, et al. A Completely Reimplemented MPI Bioinformatics Toolkit with a New HHpred Server at its Core. J Mol Biol. 2018;430(15):2237-43.
15. Fiser A, Sali A. Modeller: generation and refinement of homology-based protein structure models. Methods Enzymol. 2003;374:461-91.
16. De Lano WL. Pymol: An open-source molecular graphics tools. CCP4 Newsletter on Protein Crystallography 2002;40:82-92.

1. Squires RH, Jr., Shneider BL, Bucuvalas J, Alonso E, Sokol RJ, Narkewicz MR, et al. Acute liver failure in children: the first 348 patients in the pediatric acute liver failure study group. J Pediatr. 2006;148(5):652-8.